UNIVERSITY OF NOTTINGHAM

Metabolic signature in stage A/B heart failure: A study in asymptomatic Type 2 Diabetes

By

Emer Margaret Brady, BSc. (Hons), PhD

20416335

March 2024

Total number of words: 14,451

Dissertation submitted for the degree of Masters of Research

Table of Contents

List of Tables

List of figures

Acknowledgements

Firstly, I would like to express my sincere gratitude to my supervisors Professor David Gardner and Dr Nathan Archer for their continuous support and guidance throughout this project. Secondly, to Professor Gerry McCann for permitting me to undertake this fantastic opportunity and provide the data which embodies this work. Finally, to my husband for his unwavering support throughout the last year.

Abbreviations

BMI	Body Mass Index
CMR	Cardiac Magnetic Resonance imaging
E/e'	LV filling pressure
eGFR	estimated Glomerular Filtration Rate
FC	Fold Change
FDR	False Discovery Rate
HC	Healthy Control
HF	Heart Failure
HFpEF	Heart Failure Preserved Ejection Fraction
HFrEF	Heart Failure Reduced Ejection Fraction
HFmrEF	Heart Failure Mid-Range Ejection Fraction
HMDB	Human Metabolite Data Base
HOMA-IR	Homeostatic Model Assessment for Insulin Resistance
KEGG	Kyoto Encyclopaedia of Genes and Genomes
LV	Left Ventricular
LV CircPEDSR	LV Circumferential Peak Early Diastolic Strain rate
LV EDV	LV End Diastolic Volume
LV GCS	LV Global Longitudinal Strain
LV GLS	LV Global Circumferential Strain
LV LongPEDSR	LV Longitudinal Peak Early Diastolic Strain rate
LV mass:volume	LV mass to volume ratio
LVMI	LV mass indexed to body surface area
MPR	Myocardial perfusion reserve
MRP	Meal Replacement Plan
MSEA	Metabolite Set Enrichment Analysis
NO	Nitric Oxide
ORA	Over representation analysis
PCA	Principal Component Analysis
PLS-DA	Partial Least Squares Discriminant Analysis
SGLT2i	Sodium-Glucose co-transporter 2 inhibitors
T2D	Type 2 Diabetes

Abstract

Background: Heart failure with preserved ejection fraction (HFpEF) is a heterogenous multi-system syndrome with limited efficacious treatment options. When coupled with the rising prevalence of Type 2 diabetes (T2D), which predisposes HFpEF, it remains one of the biggest challenges in cardiovascular medicine today. Novel therapeutic targets are required to meet this important clinical need. Deep phenotyping studies including -OMIC analyses can provide important pathogenic information to aid the identification of such targets.

Aims: The overarching aim of this project is to identify and describe the metabolic signature in people with stage A/B heart failure (HF) and response to low-calorie diet.

Methods: Post-hoc analysis of a randomised controlled trial (NCT02590822) including adults with T2D and no cardiovascular disease who completed a 12-week low-energy (~810 kcal/day) meal-replacement plan (MRP) and matched healthy controls (HC). Echocardiography, cardiac MRI and fasting bloods for metabolomics were undertaken pre/post-intervention. Candidate biomarkers were identified from case-control comparison (fold change >1.5 and statistical significance $p<0.05$) and their response to the MRP reported. Association between change in biomarkers and change indices of *a*) cardiac remodelling and *b*) glycaemic control and were explored.

Results: Twenty-four people with T2D (15 males, age 51.1±5.7 years), and 25 HC (15 male, 48.3 ± 6.6 years) were included. Subjects with T2D had increased left ventricular (LV) mass:volume ratio (0.84 ± 0.13 vs. 0.70 ± 0.08, $p<0.001$), increased systolic function but impaired diastolic function compared to HC. The distinct metabolic signature was characterised by differential regulation of three key metabolic pathways; 1) glycerophospholipid metabolism, 2) sphingolipid/ceramide metabolism and 3) amino-acid metabolism namely glycine, serine and threonine metabolism. Their associated circulating plasma metabolites appear to shift towards the "*healthy status*" following significant weight-loss and normalisation of glycaemic control. However, there was no

association between the change in circulating levels of these metabolites and the change in key measures of cardiovascular structure and function nor exercise capacity following the MRP.

Conclusions: A metabolomic signature distinct from healthy controls can be described in stage A/B HF. However, this signature, despite moving towards a *'healthy status'* following the intervention is not associated with cardiac reverse remodelling. This could be attributed to the limited sample size and short exposure to the MRP and requires confirmation in larger external cohorts.

1. Introduction

1.1 Heart Failure

1.1.1 Definition, prevalence and prognosis

Heart failure (HF) is a condition whereby the heart is unable to pump enough blood around the body to meet its metabolic demands. It is a clinical syndrome resultant of structural and/or functional abnormalities of the heart and is typified by reduced exercise tolerance and symptomology of breathlessness on exertion, ankle swelling and fatigue (1). HF can be sub-divided into three types based on left ventricular ejection fraction with varying degrees of systolic or diastolic dysfunction or combinations of both (1) as summarised in Table 1.

Table 1 | European Society of Cardiology criteria for heart failure type

Type of HF		HFrEF	HFmrEF	HFpEF
CRITERIA	I	Symptoms ± Signs*	Symptoms ± Signs*	Symptoms ± Signs*
	II	LVEF≤40% Significant reduction in LV systolic function	LVEF41-49%‡ Mildly reduced LV systolic function	LVEF≥50% Significant diastolic dysfunction
	III	-	-	Objective evidence of cardiac structural and/or functional abnormalities consistent with the presence of LV diastolic dysfunction/raised LV filling pressures, including raised natriuretic peptides#

HF = heart failure; HFmrEF = heart failure with mildly reduced ejection fraction; HFpEF = heart failure with preserved ejection fraction; HFrEF = heart failure with reduced ejection fraction; LV = left ventricle; LVEF = left ventricular ejection fraction. *Signs may not be present in the early stages of HF (especially in HFpEF) and in optimally treated patients. ‡For the diagnosis of HFmrEF, the presence of other evidence of structural heart disease (e.g. increased left atrial size, LV hypertrophy or echocardiographic measures of impaired LV filling) makes the diagnosis more likely. #For the diagnosis of HFpEF, the greater the number of abnormalities present, the higher the likelihood of HFpEF.

The prevalence of heart failure in the United Kingdom is estimated at 920,000 with 200,000 new cases diagnosed annually (2). It has a huge burden on our already over stretched health service accounting for 1 million inpatient bed days and 5% of all emergency admissions to hospital, amassing costs of two billion GBP, equating to 2% of the total NHS annual budget (3). The estimated average hospitalisation is once a year after an initial HF diagnosis (4). Strong predictors of hospitalisation are co-morbidity based and include low estimated glomerular filtration rate (eGFR), increased body mass index (BMI) and poor glycaemic control as assessed by HbA1c (5). Female sex accounts for over 50% of all HF patients (2) and the prevalence increases with age, irrespective of sex, from 1% for those aged under 55 years to over 10% in the 70+ age range (6). HF continues to represent a major clinical and public health problem with an increasing prevalence trajectory (7). This is primarily driven by an aging population, increasing prevalence of co-morbidities and challenges with

efficacious and cost-effective treatment options for this complex multisystem-multi-phenotypic disease.

Overall, the prognosis of HF remains appalling with mortality rates, at 5 years post-diagnosis, estimated to be high as 50-75% (8; 9). There is a differential prognosis by type of HF with prognosis worse for those with HFrEF despite historically therapeutic trials failing to identify effective treatments for HFpEF (7; 10). The case mix of HF was generally accepted to be 50% presenting with HFrEF and the remaining with either HFmrEF or HFpEF (1). However, this continues to evolve and cases of HFpEF are now thought to predominate (11) as shown in Figure 1. This is largely attributed to our aging population and increasing prevalence of key morbidities notably the ongoing obesity pandemic (12). This is of specific concern due to the lack of disease-modifying treatments available for HFpEF.
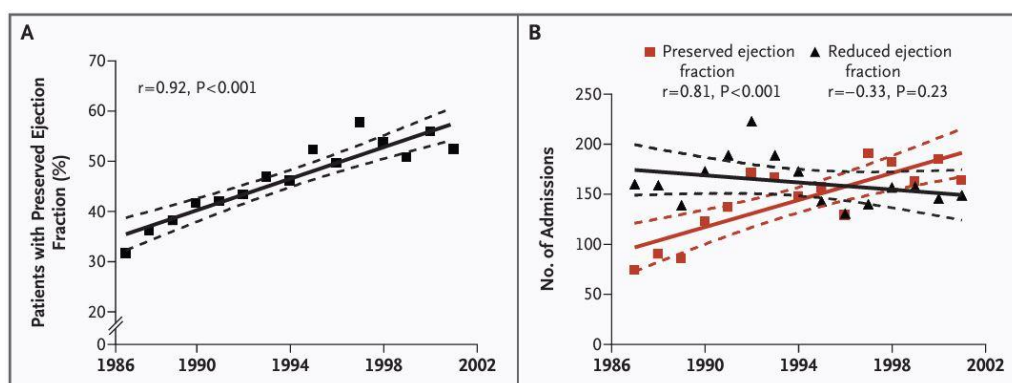
Figure 1 | Secular Trends in the Prevalence of Heart Failure with Preserved Ejection Fraction

Panel A shows the increase in the percentage of patients with HFpEF of all the consecutive patients hospitalised with decompensated heart failure at Mayo Clinic Hospitals in Olmsted County, Minnesota, between 1987 and 2001. Panel B the number of admissions for HFpEF increased, whilst those for HFrEF remained the same across the study period. The solid lines represent the regression lines for the relation between the year of admission and the percentage of patients with HFpEF (Panel A) and the number of admissions for HFpEF or HFrEF (Panel B) with 95 percent confidence intervals represented by the dashed lines. Taken form Owen T, 2006 (13).

1.2 HFpEF

HFpEF is a complex multi-organ syndrome including perturbations in the heart, vasculature, systemic metabolic and skeletal muscle, the kidney, and hepatic structural and functional changes (14). Left Ventricular (LV) ejection fraction, as previously mentioned, is preserved in HFpEF, however all these patients present with diastolic dysfunction and ventricular stiffness characterised by presence of both impaired LV active relaxation and increased passive stiffness (15; 16). Systolic dysfunction is also common in HFpEF which is subtle at rest (reduced global longitudinal strain (GLS)(17)) and pronounced on exertion (lower exercise-induced heart rate and reduced load-independent parameters of LV contractility (16)) resulting in reduced cardiac output reserve. Stiffness is not limited to the LV but encompasses other vasculature including large arteries e.g.; the aorta (18) and the myocardial microcirculation (19). Collectively, this manifests in the cardinal symptoms of HFpEF – oedema, breathlessness on exertion and exercise intolerance impacting daily living and quality of life.

1.2.1 Risk factors

The traditional and well recognised risk factors of age (1), smoking (20) and obesity (21) remain important in the development of HFpEF. Much work has been done to identify key risk factors for this multifaceted condition and to ascertain which may drive the development of HFpEF over that of HFrEF. Analysis from the Framingham Heart study identified elevated systolic blood pressure, atrial fibrillation and female sex as important multivariate predictors of HFpEF *vs*. HFrEF as shown in Figure 2 (22). In another community based study (SCREEN-HF)(23), that assessed risk factors for HFpEF, HFrEF and valvular heart failure (VHF) prior to HF diagnosis, reported hypertension, diabetes, renal dysfunction and inflammation as additional risk factors specific to HFpEF.

LBBB, 0.29 (0.16, 0.52)
IVCD, 0.54 (0.28, 1.07)
RBBB, 1.80 (1.00, 3.26)
A.Fib, 2.51 (1.66, 3.79)
BUN, 0.90 (0.80, 1.01)
Creat, 0.88 (0.73, 1.06)
K$^+$, 0.58 (0.43, 0.79)
Na$^+$, 1.07 (0.88, 1.29)
Respiratory rate, 0.81 (0.63, 1.05)
HR, 0.91 (0.84, 0.98)
DBP, 1.02 (0.97, 1.07)
SBP, 1.06 (1.00, 1.12)

0.5   1.0   1.5   2.0   2.5   3.0   3.5   4.0

Favors HFREF   Favors HFPEF   Age- and Sex-Adjusted
                                            Odds Ratio (95%CI)
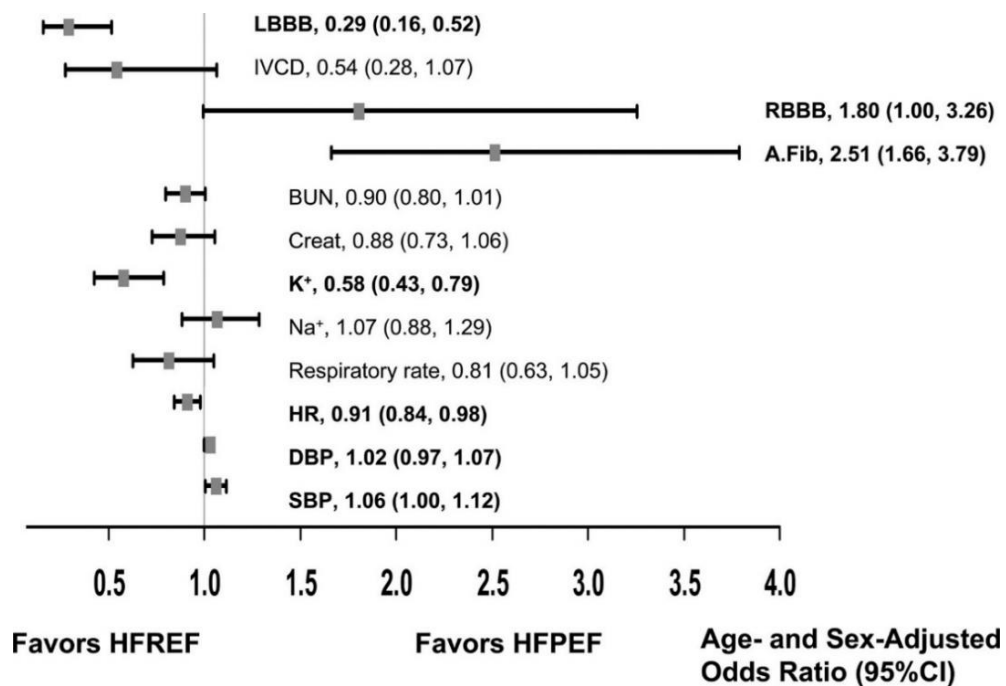
Figure 2 | Clinical risk factors associated with HFpEF or HFrEF

Figure taken from Lee, 2009 (22). Age/sex-adjusted ORs of HFpEF using pre-onset factors (OR >1: greater odds of HFpEF). ORs for age are sex adjusted, and ORs for sex are age adjusted. ORs for continuous measures are as follows: age (*per* 10 years), body mass index (BMI) (*per* 2 kg/m^2), systolic blood pressure (SBP) (*per* 10 mm Hg), diastolic blood pressure (DBP) (*per* 5 mm Hg), total cholesterol (T.Chol) (*per* 10 mg/dL), and high-density lipoprotein (HDL) cholesterol (*per* 5 mg/dL). Reference groups for categorical variables are those without the characteristic. DM indicates diabetes mellitus; HTN, hypertension

Type 2 diabetes (T2D) has been recognised as one of the most important risk factors for heart failure (HF)(24). T2D, even after the adjustment for traditional risk factors, confers a two-to-five-fold elevated risk of developing HF (25; 26). Earning its recognition as a distinct clinical entity in its own right termed 'diabetic cardiomyopathy'(27). Indeed, the recent universal guidelines for definition of HF has classified all people with T2D as Stage A "*at risk*" of HF and those with asymptomatic cardiac structural and/or functional alterations as Stage B HF (28) see Figure 3. Furthermore, people with T2D have a propensity for HF with *preserved* ejection fraction (HFpEF)(29).
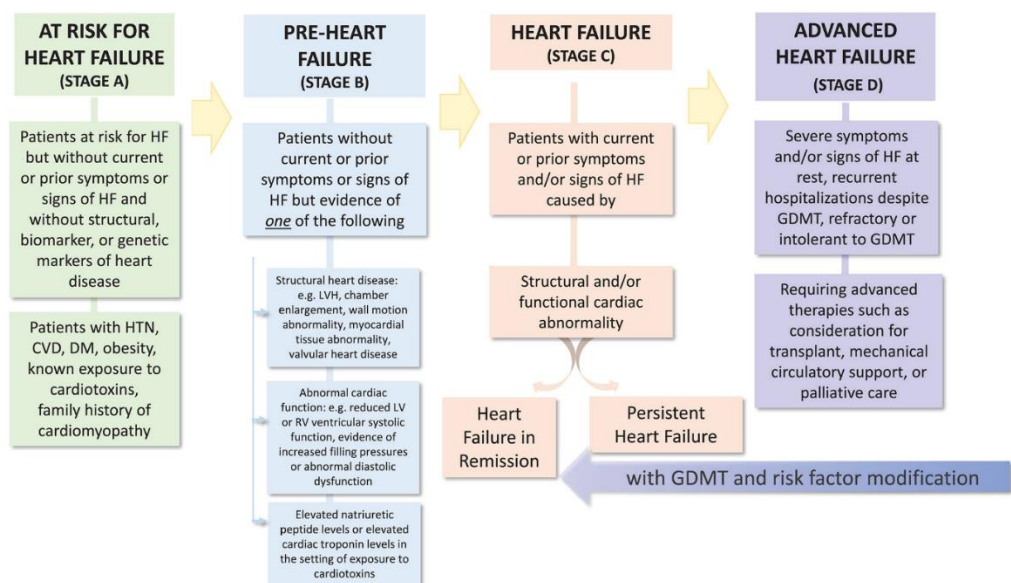
Figure 3 | The universal current approach to staging HF

Stages in the development and progression of heart failure (HF). CVD, cardiovascular disease; DM, diabetes mellitus; GDMT, guideline-directed medical therapy; HTN, hypertension; LV, left ventricular; LVH, left ventricular hypertrophy; RV, right ventricular. Taken from Bozkurt, 2021(1).

1.2.2 Diabetic cardiomyopathy

Diabetic cardiomyopathy was first described in 1972 by Rubler (30) and is defined as a cardiomyopathy observed in people with diabetes that is not attributable to hypertension, valvular or coronary artery disease or any other cardiac disease (31). The pathophysiology of this condition has been described in a number of reviews (32-34) but remains poorly understood. The recognised mechanisms to date include; fibro-inflammation, impaired Ca^{2+} handling and dysregulated myocardial energetics, which I describe in more detail below.

1.2.2.1 Fibro-inflammation

T2D is resultant from a combination of insulin resistance and reduced secretion of insulin from pancreatic islet cells. This combination gives rise to a state of chronically elevated plasma glucose levels and subsequent formation of glycated end products (AGEs) altering cellular structures and function (35). In addition, the net positive energy status of T2D leads to ectopic lipid storage and visceral adipose depots (36). This, combined metabolic load, activates

inflammatory pathways systemically and profibrotic signalling which contribute to stiffness of the left ventricle via a number of physiological processes as described in Figure 4. Moreover, our group recently demonstrated in people T2D, without cardiovascular disease, but evidence of adverse cardiovascular remodelling on magnetic resonance imaging, 20 differentially expressed biomarkers of fibro-inflammation compared to healthy controls (37). Then, following a low-calorie diet, those with T2D saw remission of their diabetes, evidence of reverse cardiac remodelling and fibro-inflammatory recovery (37).
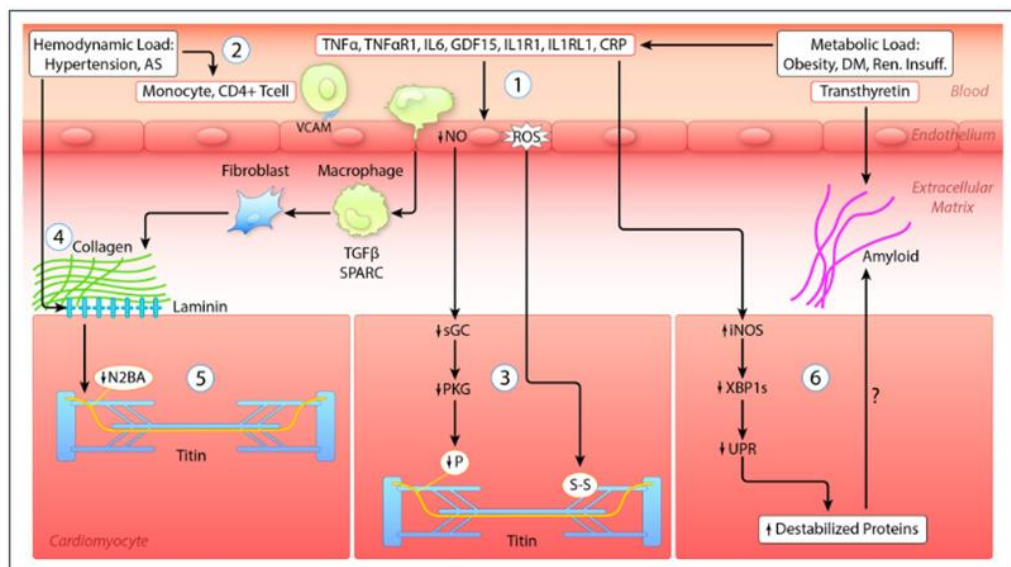
Figure 4 | Pathophysiological mechanisms linking systemic inflammation to myocardial stiffness

Taken from Paulus and Zile (38). **(1)** Metabolic load, related to diabetes (DM), and renal insufficiency (Ren Insuff) induces systemic proinflammatory signalling. Evident from raised plasma levels of TNFα (tumor necrosis factor α), TNFαR1 (tumor necrosis factor α receptor 1), IL6 (interleukin 6), GDF15 (growth differentiation factor 15), IL1R1 (interleukin 1 receptor 1), IL1RL1 (interleukin 1 receptor like 1), and CRP (C-reactive protein). Systemic inflammation triggers endothelial expression of adhesion molecules (VCAM [vascular cell adhesion molecule]), which attracts monocytes, lowers endothelial production of nitric oxide (NO), and raises endothelial production of reactive oxygen species (ROS); **(2)** hemodynamic load e.g; in arterial hypertension and aortic stenosis (AS) induces proinflammatory and fibrotic signalling evident from myocardial

infiltration of monocytes and CD4+ T cells; **(3)** low NO reduces activity of sGC (soluble guanylyl cyclase) and PKG (protein kinase G) leading to hypophosphorylation of titin (P↓). ROS causes formation of disulfide bonds within titin - raising cardiomyocyte stiffness; **(4)** myocardial collagen homeostasis: infiltrating monocytes become macrophages with production of TGFβ (transforming growth factor β) and SPARC (secreted protein acidic and rich in cysteine), which stimulate collagen production by fibroblasts; **(5)** crosstalk between hemodynamic load, extracellular matrix basal laminin, and cardiomyocyte titin results in changed titin isoform expression with lesyus N2BA isoform (N2BA↓); **(6)** myocardial accumulation of degraded proteins: expression in cardiomyocytes of iNOS (inducible nitric oxide synthase) lowers IRE1α (inositol-requiring enzyme 1α), spliced XBP1 (X-box binding protein 1), and the unfolded protein response (UPR). The latter leads to build-up of destabilized proteins, which could potentially also accumulate in the extracellular matrix as occurs in transthyretin amyloidosis (*Illustration credit: Ben Smith*).

1.1.2.3 Impaired myocardial Ca^{2+} handling

Myocardial Ca^{2+} handling has a key role in "excitation-contraction coupling" permitting normal cardiac function by modulating numerous electrophysiological processes (39). Our group, in collaboration with colleagues in Edinburgh, recently demonstrated, for the first time *in vivo,* impaired calcium handling in people with T2D without a history or symptoms of cardiovascular disease (40). In this cross-sectional study 20 cases were compared to nine healthy controls using Manganese-enhanced cardiac magnetic resonance imaging (MEMRI), a novel tool for the assessment of myocardial Ca^{2+} handling. There was a significant reduction in the uptake of myocardial manganese in people with T2D compared to controls (6.51±1.46 *vs*. 8.45±2.52 ml/100 g of tissue/min, *p*=0.003) as shown in Figure 5. This is hypothesised to be an early pathogenic feature of the diabetic heart, whereby the voltage-gated L-type calcium channels are negatively impacted by the formation of AGEs associated

with the chronic hyperglycaemic state of T2D. These calcium channels are integral to myocyte contractility and endothelial function (41).
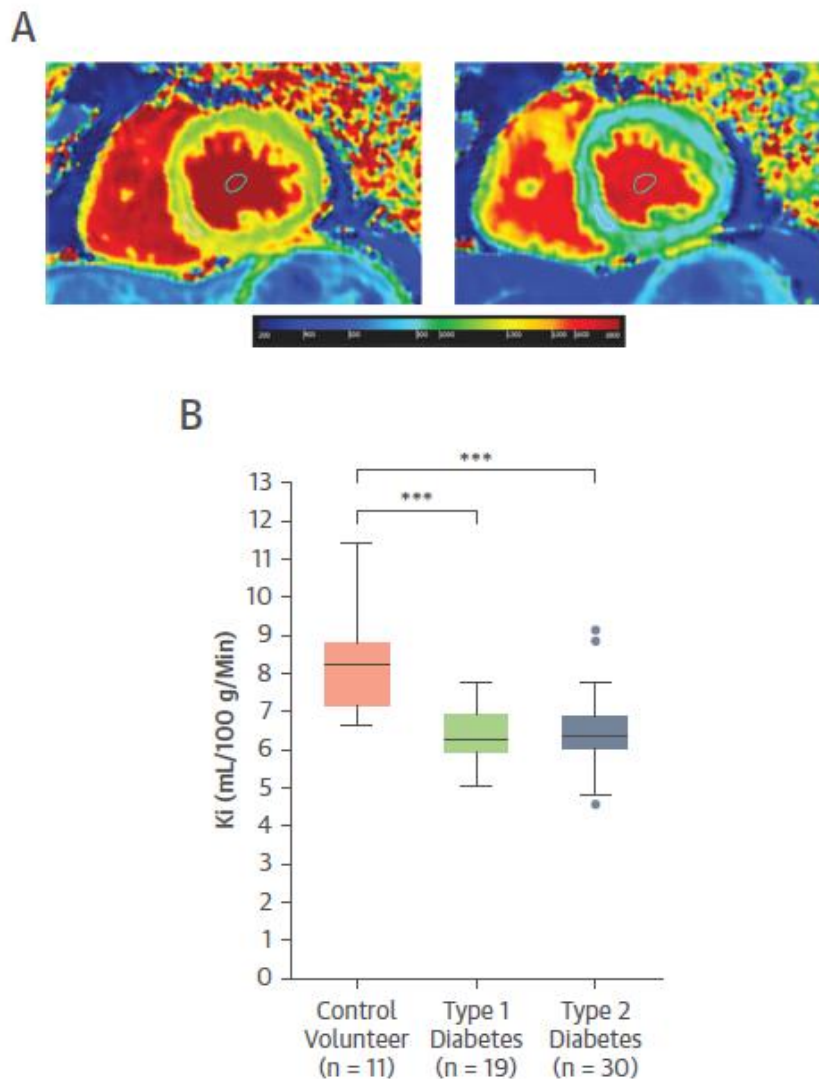
Figure 5 | MEMRI in controls, people with T2D and type 1 diabetes

Taken from Dattani.(40) (**A**) Participants underwent manganese-enhanced cardia magnetic resonance with serial T1 mapping. (**B**) People with type 1 and type 2 diabetes had lower manganese uptake (Ki) compared with control volunteers. ***P<0.001. Boxplot generated using the Tukey method.

1.1.2.4 Dysregulated myocardial energetics

The heart converts chemical energy into mechanical energy through a series of complex and tightly coordinated reactions (42). In health, the heart can metabolise a range of substrates to produce the high-energy phosphate

metabolites, adenosine triphosphate (ATP) and phosphocreatine (PCr), which are the major sources of energy for contraction and energy storage, respectively. This range of substrates includes fatty acids (FAs), glucose, amino acids and lactate. In health, the preferred substrates for ATP production are long chain FAs (60%-90%, which undergo β-oxidation) and glucose (10%-40%, via the oxidation of the pyruvate formed following glycolysis). Furthermore, under resting conditions oxidation of fatty acids amounts to ≈70% of all ATP produced, compared to increased work load e.g.; exercise, where there is a significant switch in the relative contribution of glucose to this process. To maintain consistent ATP production, it is critical to have the flexibility to utilise different fuel types for the ever-changing metabolic substrate availability and changes in metabolic demand (43). Metabolic flexibility is the ability of the body/organ to respond or adapt to changes in metabolic demand (44). In T2D, there is evidence of a reduction in the myocardial metabolic flexibility due to alterations in myocardial substrate metabolism where we see a dramatic shift away from glucose utilization with near complete reliance on FAs (43). This is postulated to play an integral role in cardiac dysfunction in T2D (45; 46).

1.3 Treatment HFpEF

The major impact for the patient with HFpEF is poor quality of life due to symptomology (47), poor mental health and inadequate 'clinical support' due to nonavailability of disease modifying treatments (48). Treatment therefore has historically been focused on treating symptoms of congestion, hypertension, encouraging weight-loss in obese-HFpEF and increasing physical activity in all patients (1). Despite this often multipronged approach outcomes remain poor, as previously discussed. However, there is early promising, yet still limited, results of new glucose lowering therapies in HFpEF. Specifically, sodium-glucose co-transporter-2 (SGLT2) inhibitors, originally developed for T2D, as evidenced by two landmark randomised controlled trials in HFpEF (EMPEROR-Preserved (49) and DELIVER (50)). Moreover, in June 2023 Dapagliflozin, an SGLT2i, was approved in the UK by NICE for the treatment of chronic HFpEF (48). However, this class of drugs do come with side-effects,

demonstrate only a modest improvement in quality of life (49; 50) and there is conflicting evidence about affordability to national health services (48; 51).

HFpEF, therefore, remains one of the biggest challenges in 21st-century cardiology and novel therapeutic targets are required to meet this important clinical need. Deep phenotyping studies including -OMIC analyses can provide information on the underpinning pathogenic mechanisms early in a disease course, track response to intervention and thus aid the identification of such targets (52). The focus of this research project is on HFpEF more specifically, to explore metabolomic signals and potential underlying pathogenic mechanisms in the early stages of HF.

2. Aims and hypothesis

2.1 Aim

The overarching aim of this project is to identify and describe the plasma metabolic signature of people with stage A/B heart failure and response to low-calorie diet. This will be achieved by addressing the following objectives;

1. Determine if the metabolic signature is different between people with stage A/B heart failure and matched healthy controls
2. Identify specific metabolic pathways that are differentially regulated in Stage A/B HF
3. Following significant weight-loss via a low-calorie diet does the metabolic signature move towards the healthy status
4. Determine which metabolites are associated with indices of cardiovascular structure and function

2.2 Hypotheses

1. There will be a distinct metabolic signature in people with stage A/B HF described by the differential expression of multiple metabolites
2. The stage A/B HF metabolic signature will shift towards the healthy status following the 12-week MRP
3. Specific metabolic pathways will be associated with measures of cardiovascular remodelling i.e., mass:volume ratio

3. Methods

3.1 Study participants

The data for the analysis within this project were derived from the Diabetes Interventional Assessment of Slimming or Training tO Lessen Inconspicuous Cardiovascular Dysfunction (DIASTOLIC) trial (53). DIASTOLIC was a prospective, randomised, open-label, blinded end-point trial that assessed the effects of a 12-week intervention with either: 1) supervised aerobic exercise thrice weekly, 2) a nutritionally complete low-energy Meal Replacement Plan (MRP), or 3) routine care with standard lifestyle advice on sub-clinical cardiac dysfunction. Detailed inclusion/exclusion criteria are published (51; 53) and summarised in Table 2. Participants were randomised (1:1:1) to each group. Random allocation was stratified by sex and baseline glucose lowering therapy and conducted by an independent online-computerized randomization system incorporating concealed allocation (Sealed Envelope). At baseline, age-, sex- and ethnicity-matched healthy controls were enrolled for case-control comparisons. The study protocol and the primary results of the trial have been previously published. The study received ethical approval by the National Research Ethics Service (15/WM/0222) and is registered with www.clinicaltrials.gov (NCT02590822). Only data for the MRP and healthy controls are included in this project as detailed in the study consort diagram in Figure 6. Data were collected at 0- and 12-weeks post intervention and only after participants gave informed consent.

Table 2 | Summary inclusion and exclusion criteria for the DIASTOLIC study

Inclusion criteria	Exclusion Criteria
Established T2D (≥ 3months)	T2D duration >12 years
HbA1c ≤9%if on triple therapy or ≤10%on diet and exercise or monotherapy or dual therapy	Taking > 3 glucose lowering therapies
Current glucose-lowering therapy either mono, dual or triple of any combination of metformin, sulphonylurea, DPP-IV inhibitor, GLP-1 therapy or an SGLT2i± diet and exercise	Known macrovascular disease including coronary artery disease, stroke/TIA or peripheral vascular disease
BMI >30kg/m2 or >27kg/m2 (South Asian).	Presence of arrhythmia (including atrial fibrillation, atrial flutter or second- or third-degree atrioventricular block)
Diagnosis of T2D before the age of 60years of age.	Known heart failure or other clinically relevant heart disease
Working aged adults (≥18and ≤65years)	Weight loss >5kg in preceding 6 months
	Cardiovascular symptoms (angina and limiting dyspnoea during normal physical activity
	Stage 4 or 5 chronic kidney disease (eGFR <30mL/min/1.73m^2)
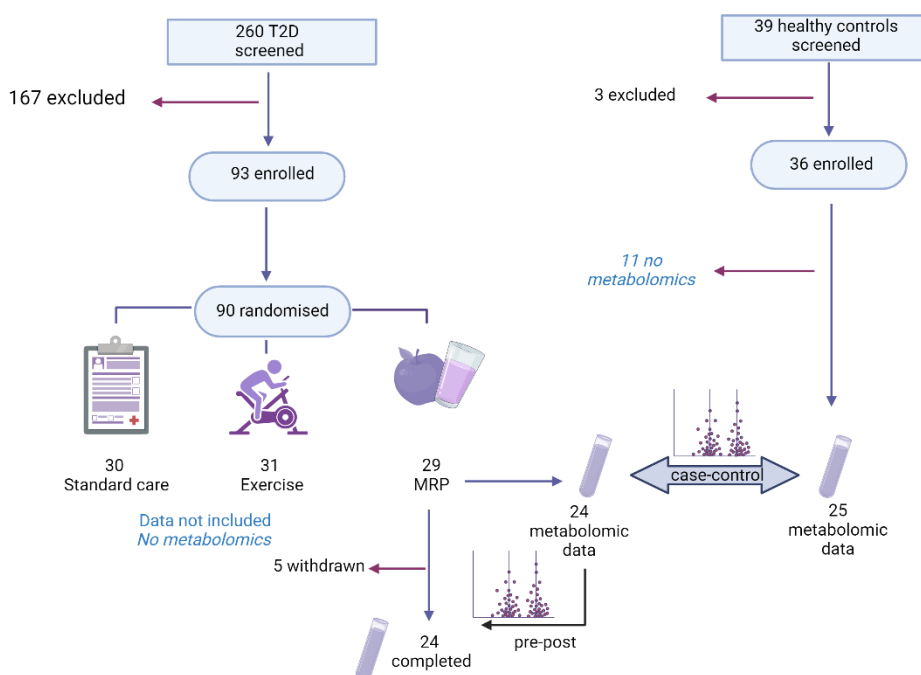
Figure 6 | Study consort

3.3 Low energy meal replacement plan (MRP)

The low energy meal replacement plan was provided by Cambridge weight plan and complied with guidance and government legislation (European Food safety authority)(54) at point of study delivery. In summary, it contained an average of ≈810 kcal/day (30% protein, 50% carbohydrate, 20%) in the form of shakes, bars, soups and snacks with an advisory 2litres of non-calorific fluid/day. Non-starchy vegetables could also be added to a meal for added texture and bulk. Abstinence from alcohol was required in addition to a continuation of normal levels of physical activity. The MRP was supported with health behaviour coaching and relapse prevention with weekly contact by a qualified dietician or equivalent *as per* the individual needs of the participant. Non-compliance triggered withdrawal from the study and was defined as failing to achieve a loss of >2% body weight at week 1 and 4% at week 3. When 50% excess body weight was lost or when the participant reached the end of intervention period (12 weeks) food was reintroduced by way of a maintenance diet individualised to and agreed with the participant by the study dietician.

At point of diet initiation all glucose-lowering therapies and antihypertensive drugs were discontinued to avoid hypoglycaemia and hypotension, respectively.

3.3 Study Assessments (Figure 7)
3.3.1 Cardiometabolic and participant characteristics

Demographics, medical history, and anthropometric measures including Dual-energy X-ray Absorptiometry (DEXA) for body composition were collected. Participants fasted overnight and took their morning medication(s) after the study visit. Their last meal was not standardised. Fasting blood samples were obtained and the residual supernatant plasma stored at -80˚C prior to batch analysis. HbA1c, glucose, liver, kidney function and lipid profile were analysed according to standard operating procedures in the accredited laboratory at University Hospitals Leicester, NHS Trust. Insulin was quantified by multiplex assay on a Luminex platform. A further sample was taken for plasma to be

extracted at source and then stored at -80°C for further analysis which included metabolomic analysis. Blood pressure was taken seated after five minutes rest on three occasions with the mean of the final two readings reported.

3.3.2 Cardiac MRI

MRI scans were conducted on a 1.5T platform (MAGNETOM Aera; Siemens, Erlangen, Germany) with methods previously described (53). To note all images were analysed offline blinded to treatment group. The MRI outcomes of interest were selected to permit investigation of cardiovascular structure and function and included; LV End Diastolic Volume (LV EDV (ml)), LV mass indexed to body surface area, (LVMI, g/m2), LV mass to volume ratio (LV mass/volume (g/mL), LV Global Longitudinal Strain (LV GLS (%)), LV Global Circumferential Strain (LV GCS (%)), LV Longitudinal Peak Early Diastolic Strain rate (LV LongPEDSR (s-1)), LV Circumferential Peak Early Diastolic Strain rate (LV CircPEDSR (s-1)) and myocardial perfusion reserve (MPR).

3.3.3 Transthoracic Echocardiography

Echocardiography was performed and interpreted by two accredited operators using an iE33 system with S5-1 transducer (Philips Medical Systems, Best, the Netherlands) to estimate Left Ventricular (LV) filling pressures (E/e').

3.3.4 Cardiopulmonary Exercise testing (CPET)

Exercise tolerance was assessed by a symptom-limited maximum incremental exercise test on a stationary bicycle (electromagnetically braked cycle ergometer) with expired gas analysis to determine $\dot{V}O_2$peak in a temperature-controlled laboratory.

3.3.5 Metabolon Platform

A plasma sample from the healthy controls at baseline and a pre- and post-intervention sample, from the participants randomised to the MRP, were sent to an external company Metabolon, Inc for metabolomic profiling (North Carolina, USA, http://www.metabolon.com/). The following sub-sections describe their sample preparation, quality control and mass spectrometry methodology as was provided by Metabolon.

3.3.5.1 Sample Preparation

Samples were prepared using a Hamilton automated MicroLab STAR® system. For quality control (QC) several recovery standards were added prior to the first step of the extraction process. To remove protein, dissociate small molecules bound to protein or trapped in the precipitated protein matrix, and to recover chemically diverse metabolites, proteins were precipitated with methanol under vigorous shaking for 2 min (Glen Mills GenoGrinder 2000) followed by centrifugation. The resulting extract was then divided into five fractions: two for analysis by two separate reverse phase (RP)/UPLC-MS/MS methods with positive ion mode electrospray ionization (ESI), one for analysis by RP/UPLC-MS/MS with negative ion mode ESI, one for analysis by HILIC/UPLC-MS/MS with negative ion mode ESI, and one sample held back as a spare. TO remove any organic solvents samples were placed briefly on a TurboVap® (Zymark). The sample extracts were then stored overnight under nitrogen before preparation for analysis.

3.3.5.2 Quality assurance and quality control

Several types of controls were analysed in concert with the experimental samples: a pooled matrix sample generated by taking a small volume of each experimental sample (or alternatively, use of a pool of well-characterized human plasma) served as a technical replicate throughout the data set; extracted water samples served as process blanks; and a cocktail of QC standards that were carefully chosen not to interfere with the measurement of endogenous compounds were spiked into every analysed sample, allowed instrument performance monitoring and aided chromatographic alignment. Instrument variability was determined by calculating the median relative standard deviation (RSD) for the standards that were added to each sample prior to injection into the mass spectrometers. Overall process variability was determined by calculating the median RSD for all endogenous metabolites (i.e., non-instrument standards) present in 100% of the pooled matrix samples. The instrument variability for the internal standards was 4% and the total process

variability for the endogenous biochemicals was 7%, both of which met metabolons quality threshold. Finally, the experimental samples were randomised across the platform run with QC samples spaced evenly among the injections.

3.3.5.3 Mass Spectroscopy at metabolon

The Waters ACQUITY ultra-performance liquid chromatography (UPLC) and a Thermo Scientific Q-Exactive high resolution/accurate mass spectrometer interfaced with a heated electrospray ionization (HESI-II) source and Orbitrap mass analyser operated at 35,000 mass resolution were used for these analyses. All analysis were blinded to clinical data and is described below.

The sample extracts were dried then reconstituted in solvents compatible to each of the four analysis methods detailed below. Each reconstitution solvent contained a series of standards at fixed concentrations to ensure injection and chromatographic consistency.

- One aliquot was analysed using acidic positive ion conditions, chromatographically optimized for more hydrophilic compounds. In this method, the extract was gradient eluted from a C18 column (Waters UPLC BEH C18-2.1x100 mm, 1.7 µm) using water and methanol, containing 0.05% perfluoropentanoic acid (PFPA) and 0.1% formic acid (FA).

- The second aliquot was also analysed using acidic positive ion conditions, but chromatographically optimized for more hydrophobic compounds. In this method, the extract was gradient eluted from the same C18 column using methanol, acetonitrile, water, 0.05% PFPA and 0.01% FA and was operated at an overall higher organic content.

- A third aliquot was analysed using basic negative ion optimised conditions using a separate dedicated C18 column. The basic extracts were gradient eluted from the column using methanol and water, however with 6.5mM Ammonium Bicarbonate at pH 8.

- The fourth aliquot was analysed via negative ionization following elution from a HILIC column (Waters UPLC BEH Amide 2.1x150 mm, 1.7 μm) using a gradient consisting of water and acetonitrile with 10mM Ammonium Formate, pH 10.8.

The MS analysis alternated between MS and data-dependent MS^n scans using dynamic exclusion. The scan range covered 70-1000 m/z (mass to charge ratio).

3.3.5.4 Data Extraction and Compound Identification at Metabolon

Raw data was extracted, peak-identified and QC processed using Metabolon's hardware and software. These systems are built on a web-service platform utilizing Microsoft's .NET technologies, which run on high-performance application servers and fiber-channel storage arrays in clusters to provide active failover and load-balancing. Compounds were identified by comparison to library entries of purified standards or recurrent unknown entities. Metabolon maintains a library based on authenticated standards that contains the retention time/index (RI), mass to charge ratio (m/z), and chromatographic data (including MS/MS spectral data) on all molecules present in the library. Furthermore, biochemical identifications are based on three criteria: RI within a narrow RI window of the proposed identification, accurate mass match to the library +/- 10 ppm, and the MS/MS forward and reverse scores between the experimental data and authentic standards. The MS/MS scores are based on a comparison of the ions present in the experimental spectrum to the ions present in the library spectrum. While there may be similarities between these molecules based on one of these factors, the use of all three data points can be utilized to distinguish and differentiate biochemicals. More than 3300 commercially available purified standard compounds have been acquired and registered into LIMS for analysis on all platforms for determination of their analytical characteristics. Additional mass spectral entries were created for structurally unnamed biochemicals, which were identified by virtue of their recurrent nature (both chromatographic and mass spectral). These compounds

have the potential to be identified by future acquisition of a matching purified standard or by classical structural analysis.

The QC and curation processes were designed to ensure accurate and consistent identification of true chemical entities, and to remove those representing system artifacts, mis-assignments, and background noise. Metabolon data analysts use proprietary visualization and interpretation software to confirm the consistency of peak identification among the various samples. Library matches for each compound were checked for each sample and corrected if necessary. The resulting clean dataset was then transferred to the research team with annotations for compound identity which included * to denote a compound that was not confirmed based on a standard, but Metabolon were confident in its identity and ** which denoted compounds for which a standard is not available, but Metabolon were reasonably confident in its identity or the information provided. All others i.e.; with no annotation Metabolon were confident of the metabolites identity based on three criteria detailed above.
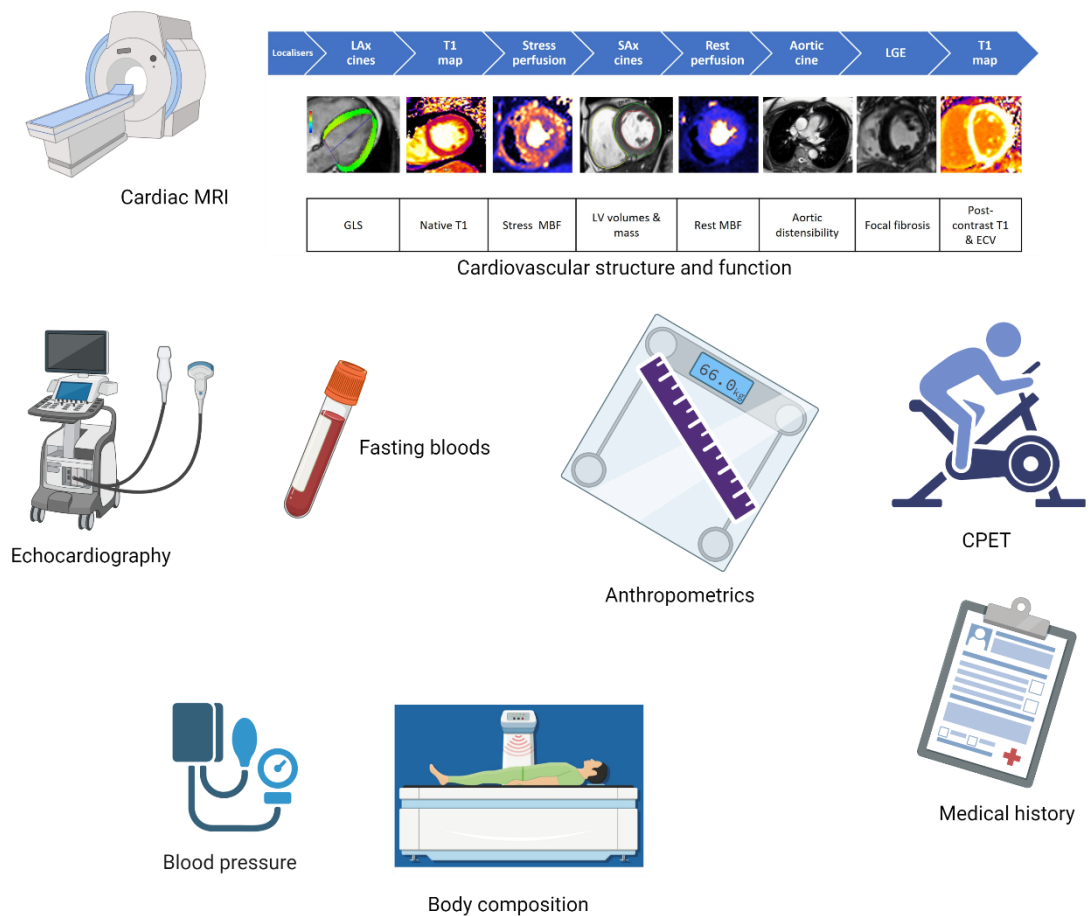
Figure 7 | Study assessments undertaken in DIASTOLIC trial

3.4 Data Analysis

3.4.1 Data pre-processing

The metabolomic data used in this project was the original scaled data in the form of compound signal intensity lists, provided by Metabolon in an excel spreadsheet (pre-processed). The clinical data generated from the DIASTOLIC trial was provided in an excel spreadsheet for the whole DIASTOLIC randomised controlled trial. The two datasets required cleaning. Firstly, the clinical dataset was restricted to only those who completed the MRP intervention and those healthy controls who had plasma samples processed for metabolomics. All variables were checked for erroneous entries and relabelled for ease of interpretation and satisfaction of analysis software requirements.

Missing data were assessed 1) missing metabolomic data were identified by *MetaboAnalyst* and replaced with 1/5th the minimum positive value for the given metabolite, 2) missing clinical data were identified by group *per* variable and the mean or median (whichever was appropriate based on data distribution) for the that variable, for the given group, was calculated and replaced said missing value.

Metabolites that were not considered meaningful or of relevance were removed. This included metformin and three ibuprofen metabolites. Metformin was removed because it is second line therapy for T2D and only those with T2D were taking this drug at baseline (all participants bar one), furthermore all glucose lowering medication was stopped at point of starting MRP as previously mentioned, therefore this metabolite would likely be identified as a candidate biomarker in error. The three ibuprofen metabolites were removed, given pain relief medication was not part of the research questions for this project. These metabolites were not annotated with * or ** and therefore Metabolon were confident in their identity based on their RI, accurate mass match to their spectral library +/- 10 ppm, and the MS/MS forward and reverse scores between the experimental data and authentic standards.

The data were then split into two separate files 1) case-control only, 2) pre-, post metabolomics data only. Then an additional two datasets were created where I merged the clinical data with the metabolites for case-control only and pre-, post data only.

3.4.2 Cohort characteristics

The distribution of the clinical data were assessed for normality visually using histograms and Q-Q plots and statistically using Shapiro Wilk test of normality. Continuous data are reported as mean (± standard deviation (SD)) if normally distributed or median (interquartile range (IQR)) where not. Categorical data reported as count (percentage). Demographic and standard clinical characteristics between the cases (T2D) and controls are described without testing for statistical significance given these were not specific aims being

assessed. For measures of cardiovascular structure and function, between groups were tested using independent t-test and Mann-Whitney U as appropriate. These data were analysed in IBM SPSS Statistics for Windows, Version 26.0.

3.4.3 Candidate biomarker identification

The metabolomic data were analysed using the web-interface *MetaboAnalyst*, version 5.0 (55).

3.4.3.1 Case-control

The data were formatted in a data matrix appropriate for one-factor statistical analysis in *MetaboAnalyst* and missing data handled as described above. The data filtering step identifies and removes variables that are unlikely to be meaningful and of use to modelling. However, the data had already been filtered by metabolon therefore this step was not undertaken. The complete dataset was then normalised (to remove unwanted variation) by sum; that is, each metabolite value is divided by the total sum for that metabolite count and multiplied by 100.   It was then log10 transformed to provide an improved data distribution. The dataset was visualised by principal component analysis and partial least squares discriminant analysis. The fold-change (FC) between case and controls were then calculated. A volcano plot was created with FC set at 1.5 and adjustment for false discovery rate (FDR) to identify potential candidate biomarkers.

Once the candidate biomarkers were identified a truncated dataset containing just these was produced. The compound identifier (HMDB ID) for each metabolite was found via the Human Metabolome Database (https://hmdb.ca/) and added to each biomarker. This dataset was then uploaded to *MetaboAnalyst* for enrichment and pathway analysis. The parameters set for the pathway analysis are listed in Table 3.

Table 3 | Analysis parameters set for pathway analysis in MetaboAnalyst

Parameter	Selected	Detail
Visualisation Method	Scatterplot	Output for pathway impact
Enrichment method	Hypergeometric	A one-sided test that tests whether the pathway is enriched/over-represented within the list of most significantly associated metabolites within the group of interest – utilising the geometric distribution
Topology Analysis	Relative betweeness centrality	Betweenness centrality measures the amount of information streaming through a given node
Reference metabolome	Use all in library: Homosapiens (KEGG)	Humans in the "Kyoto Encyclopedia of Genes and Genomes" database

A heatmap was created to highlight which of the identified biomarkers had a role in the dysregulated biological pathways identified from the pathway analysis.

The Metabolite Set Enrichment Analysis (MSEA) module within *MetaboAnalyst* is a way to identify biologically meaningful patterns that are significantly enriched in quantitative metabolomics. This module takes the metabolites from the list provided and assesses if they are functionally related without requirement of a concentration and arbitrary threshold of significance. The metabolite library selected was KEGG which had (at time of analysis) 84 metabolite sets based on KEGG human metabolic pathways. Only metabolite sets containing at least two entries were considered. Over representation analysis (ORA) was conducted using the hypergeometric test with adjustment for multiple testing. This evaluates if a specific set of metabolites are represented more than would be expected by chance within the compound list provided.

To determine if or which of the candidate biomarkers were related to the nine cardiovascular outcomes of interest a correlation analysis was undertaken. Data were loaded into R-studio and a correlation matrix was produced. A plot was created for each CMR variable and peak VO_2 separately displaying the top 20 correlation variables with a $p<0.05$ (total of nine plots). A data reduction step followed whereby only those biomarkers identified with a significant

correlation with ≥ 1 outcome of interest were taken forward. Using "corrplot" package a correlograms with pie-charts representing the direction and strength of the correlation were created for the first 10 candidate biomarkers, followed by the second and so on. The data were split this way to aid interpretation of the visualisation.

3.4.3.2 Pre-, post-MRP

The first step with this dataset was data visualisation using principal component and partial least squares discriminant analysis and a heat map with hierarchical clustering in *MetaboAnalyst*. Then the same method for candidate biomarker identification used in the case-control was followed for the pre-, and post-MRP dataset using *MetaboAnalyst* but selecting 'paired analysis' because the two groups are related. Once the candidate biomarkers were identified a truncated dataset containing just these were produced with their corresponding HMDB IDs. A data reduction step followed whereby only those biomarkers common across both analyses were taken forwards. The raw count data for the selected biomarkers for pre-, post-MRP and healthy controls were merged and box-plots produced, using the Tukey method, to visualise the change/difference in the levels of each metabolite between the three groups. The plots were generated using GraphPad Prism version 9.0.0 for Windows, GraphPad Software, San Diego, California USA, www.graphpad.com.

The change in metabolite concentration (signal intensity) was then calculated (subtracting pre-MRP results from post-MRP results). The change in the remaining outcomes of interest were calculated in the same manner and the datasets merged to create a 'change' dataset. Using "corrplot" package in R studio again correlograms were created but this time using the circle method and display of correlation co-efficients for ONLY those that met a significance of $p < 0.01$. This permitted visualisation and assessment of relationships between 1) candidate biomarkers and outcomes of interest, and 2) candidate biomarkers and key metabolic indices. Scatter plots were then produced for any correlations that were considered of potential relevant i.e.; $r > 0.05$ and $p < 0.005$ using Base R in R studio.

4. Results

4.1 Case-control

Twenty-nine asymptomatic T2D participants (cases) were randomised to the MRP group with 24 completing the study with metabolomics data. Twenty matched controls (age, sex and ethnicity) were selected for metabolomics analysis (Figure 6). The baseline characteristics by group are provided in Table 4.

Table 4 | Baseline characteristics table for cases and control

Variable	Cases (T2D) N=24	Controls (Healthy) N=25	
Clinical characteristics			
Age (years)	51.1 ± 5.7	48.3 ± 6.6	
Sex (M (%))	15 (63)	15 (60)	
Ethnicity (WE (%))	15 (63)	17 (68)	
Weight (kg)	106.7 ± 16.2	69.9 ± 11.4	
BMI (kg/m2)	37.4 ± 5.9	24.3 ± 2.5	
Systolic BP (mmHg)	145.9 ± 15.9	118.4 ± 10.7	
Diastolic BP (mmHg)	91.1 ± 7.4	76.2 ± 6.0	
Heart rate (bpm)	73.1 ± 8.6	61.8 ± 9.3	
HbA1c (%)	7.2 ± 1.1	5.4 ± 0.2	
HbA1c (mmol/mol)	54.8 ± 11.9	35.6 ± 2.6	
HOMA-IR	12.2 ± 8.2	2.0 ± 1.9	
Medical history			
Duration diabetes (m)	58.3 ± 39.8	-	
Smoking history (yes)	10 (41)	7 (28)	
Hypertension (n (%))	15 (63)	0 (0)	
Hypercholesterolemia (n (%))	16 (67)	0 (0)	
Cardiovascular Imaging			*p* value
LV Massi (g/m²)	58.2 ± 9.8	57.8 ± 13.1	0.902
LV EDVi (mL/m²)	69.9 ± 11.3	82.9 ± 18.0	**0.004**
LV mass:volume (g/mL)	0.84 ± 0.13	0.70 ± 0.08	**<0.001**
LV EF (%)	70.0 ± 7.4	64.7 ± 4.9	0.005
LV GLS (%)	16.6 ± 2.8	17.6 ± 1.5	0.108
LV GCS (%)	21.0 ± 2.3	19.6 ± 2.0	**0.029**
LV LongPEDSR (s-1)	0.79 ± 0.15	0.89 ± 0.16	**0.021**
LV CircPEDSR (s-1)	1.00 ± 0.20	1.10 ± 0.16	0.060
LA EF (%)	55.0 ± 7.7	59.1 ± 7.8	0.075
Mean Ao Distens (mmHg⁻¹x10⁻³)	3.7 ± 1.9	6.9 ± 2.0	**<0.001**
MPR	3.0 ± 1.0	4.2 ± 1.0	**<0.001**
Average E/e'*	9.4 (4.5)	5.9 (2.6)	**<0.001**
Cardiopulmonary exercise testing			
Peak VO2 (mL/kg/min)	16.4 ± 4.47	28.76	**<0.001**

Abbreviations: BMI = body mass index, LV EF = Left ventricular ejection fraction, LV Massi = Left Ventricular Mass Indexed for body surface area, mass:volume = mass to volume ratio , LV EDVi = Left Ventricular End Diastolic Volume indexed for height, GLS = global longitudinal strain, LongPEDSR = Longitudinal Peak Early Diastolic Strain rate, CircPEDSR = Circumferential Peak Early Diastolic Strain Rate, GCS = global circumferential strain, LAVImax = Left atrial maximum volume indexed for body surface area, Mean Ao Distens = Mean aortic distensibility, MPR= Myocardial perfusion reserve. Data are reported as mean ± standard deviation, count (percent) or median (interquartile range). Bold font highlights statistically significant difference with significance level of 95%.

At baseline, as expected, cases had higher body weight, blood pressure, HbA1c and level of insulin resistance with over half having hypertension and high cholesterol compared to none in the healthy group. Diabetes medication included one person with diet and lifestyle only (4%), 18 (75%) on monotherapy, three (13%) on dual therapy and two (8%) on triple therapy. No patients were taking insulin and only one and two were on Glucagon Like Peptide-1-Receptor agonists or SGLT2i, respectively. None of the healthy controls were taking any medication.

There was evidence of cardiovascular remodelling in those with T2D who had significantly lower left ventricular volume, higher mass:volume ratio with higher ejection fraction and global strain but worse diastolic function (LV filling pressures (E/é) and peak early diastolic strain rate). In addition, there was decreased aortic distensibility and lower myocardial perfusion reserve in T2D compared to the controls.

4.1.1 Candidate biomarkers

The metabolon platform returned 851 compounds of known identity (named biochemicals). After removal of the four nonsense metabolites there remained 847 compounds for the 49 samples comprising the two-groups. *MetaboAnalyst* identified and removed five features with a constant/single value across samples. A total of 3461 (8.6%) of data were identified as missing and replaced as previously described.

After applying the normalisation step the data were better standardised across the metabolites as demonstrated by comparing the before and after normalisation density curves and box plots as seen in Appendix 1.

The three-dimensional PCA score plot based on _all_ of the metabolites identified by Metabolon is displayed in Figure 8. The plot demonstrates reasonable-to-good separation between those with T2D and the healthy group based on their metabolomic profiles. The two-dimensional PLS-DA score plot with predictive component 1 and component 2 better demonstrates discrimination of the two groups due to variation in their metabolic profiles demonstrated in plot B of

Figure 8 and finally the group separation is best visualised by the PLS-DA 3D-plot seen in plot C of this figure.
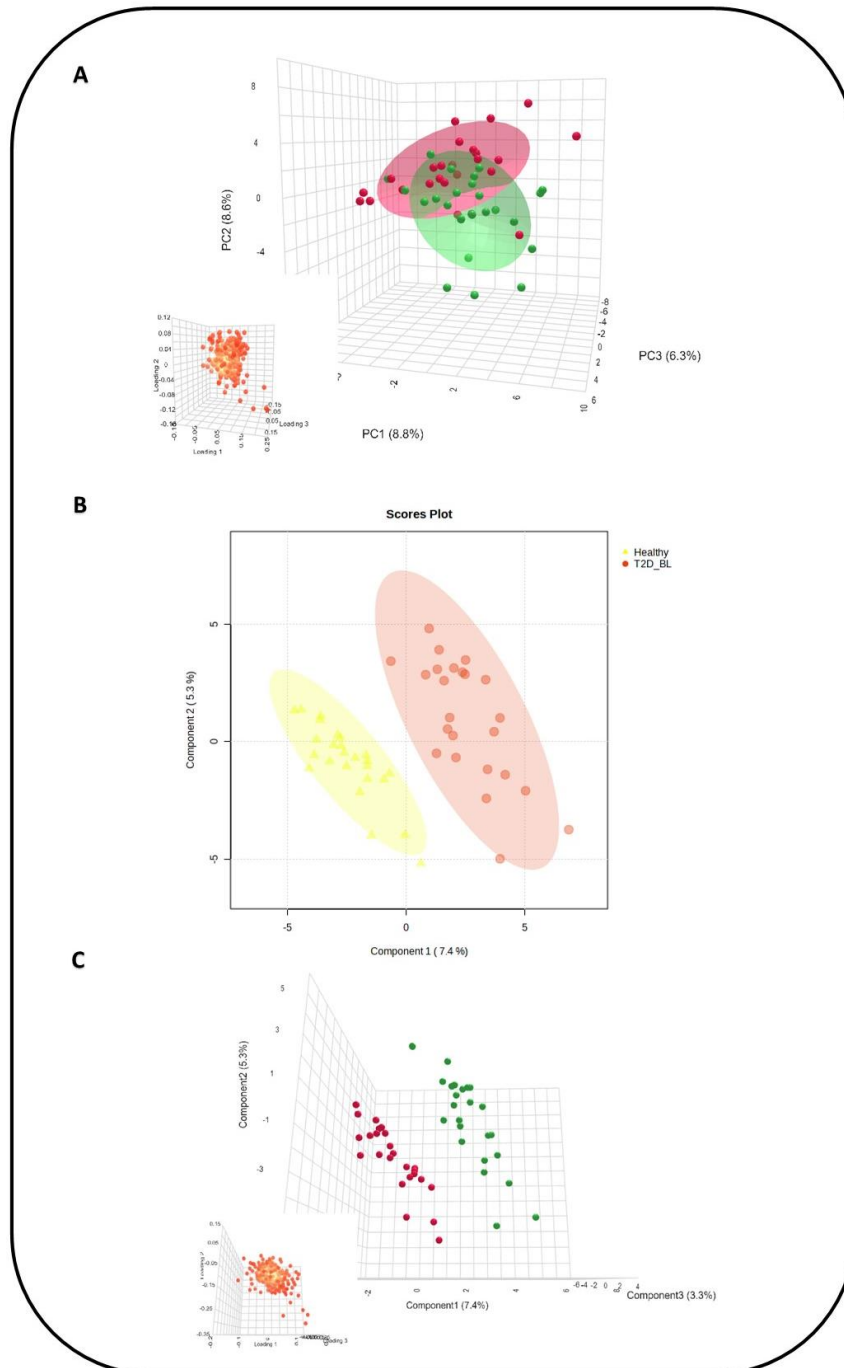
Figure 8 | Principal component and partial least squares discriminant analysis plots (outputs from MetaboAnalyst)

Plot A: 3D Principal component analysis plot with the first three principal components collectively accounting for 23.7% of the variation within the

dataset. Plot B: 2D partial least squares discriminant plot with first two predictive components and Plot C: 3D partial least squares discriminant plot with first three predictive components.

The Q^2 value for 2 and 3 components were 0.71 and 0.70, respectively, and the corresponding R^2 values were 0.89 and 0.93, respectively, further indicating good predictive power of the model. The empirical *p* value for the permutation test was $p < 0.01$ for 100 permutations and $p < 5e\text{-}04$ for 2000 permutations indicating that the null hypothesis can be rejected and thus confirms evidence of a difference between the two groups.

A FC identified between cases-controls was identified in a total of 193 metabolites (102 downregulated and 91 upregulate as shown in Figure 9. Of these a total of 94 had a FC≥ 1.5 with adjustment for FDR meeting the threshold for statistical significance (*p*<0.05) as presented in Figure 10, with 43 downregulated and 51 upregulated (Appendix 3). The dysregulation of amino acid and lipid pathways are dominant; for those downregulated 33% (14/43) belonged to amino acid pathways and 44% (19/43) to lipid pathways, for those upregulated 16% were amino acid pathways and 61% (31/51) lipid pathways. The HMDB compound ID could only be identified for 92 metabolites and therefore 92 were taken forward for pathway analysis.
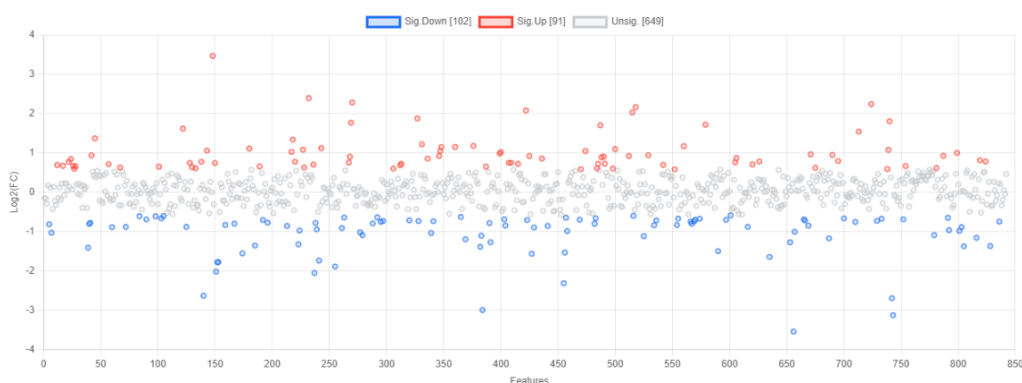
Figure 9 | Scatter plot for fold-change between case-controls across 847 metabolites (MetaboAnalyst output)

For both plots each circle represents a metabolite with those coloured blue = significantly downregulated in cases *vs*. control, red = significantly up regulated

in cases *vs*. control and grey = no significant fold change between cases and control.
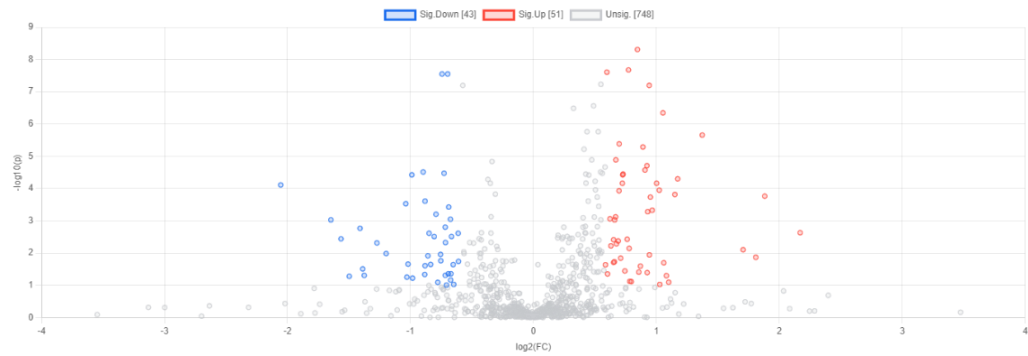
Figure 10 | Volcano plot identifying biomarkers with a significant fold-change adjusted FDR (MetaboAnalyst output)

4.1.3 Enrichment analysis

The HMDB IDs for the original 92 candidate biomarkers were uploaded into the enrichment module in *MetaboAnalyst*. Twenty metabolites were not recognised by the reference library and were subsequently removed. The plot in Figure 11 represents the top 25 enriched pathways with their associated enrichment ratios in a bar chart and dot plot. The enrichment ratio is the number of hits within a recognised metabolic pathway divided by the expected number of hits. The top five metabolic pathways with statistically significant high enrichment ratios are all amino-acid metabolic pathways, indeed across the total top 25 pathways that are overrepresented within the cases, amino acid metabolism is heavily represented.
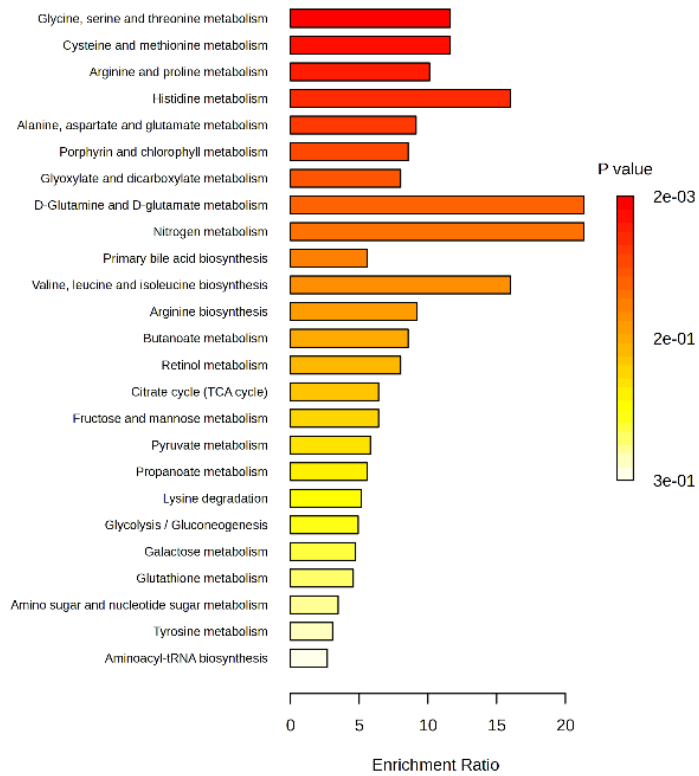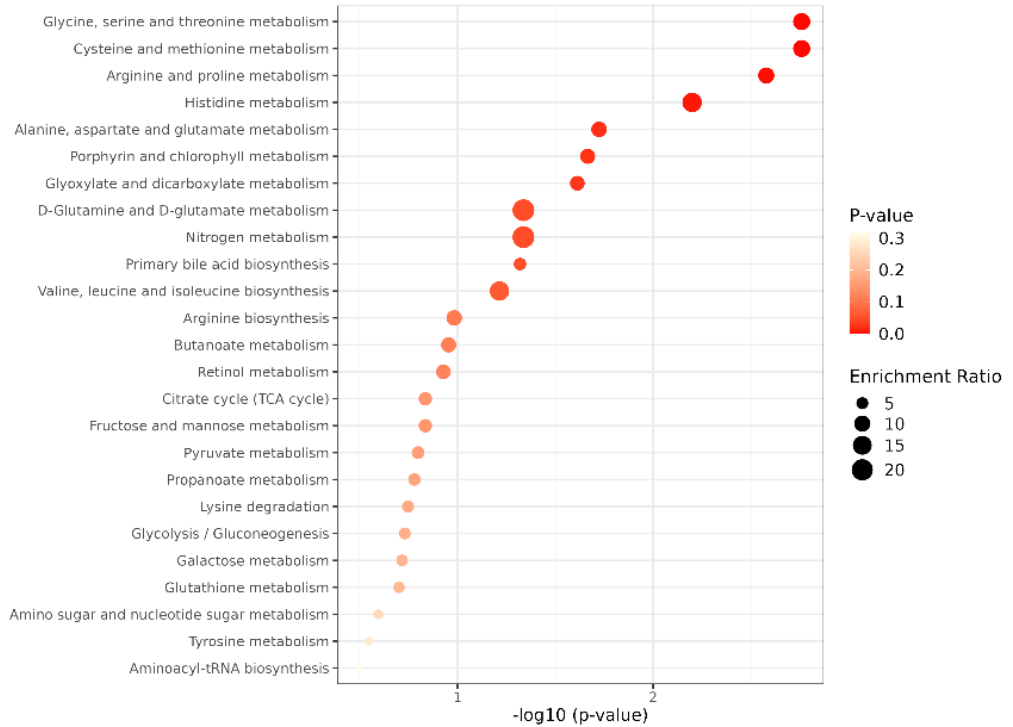
Figure 11 | Overview of enriched sets of metabolites (outputs from MetaboAnalyst)

The top panel provides the bar chart and bottom the dot plot showing the top 25 enriched pathways.

4.1.2 Pathway analysis

The list of HMDB compound names were uploaded into *MetaboAnalyst* for pathway analysis. The same 20 compounds, as for the enrichment analysis, were not recognised in the selected human metabolome reference library. These were subsequently removed and 28 pathways were identified as different between cases and controls. An overview of the pathway analysis with the relative impact of each pathway and a list of identified dysregulated pathways is provided in Figure 12 below.
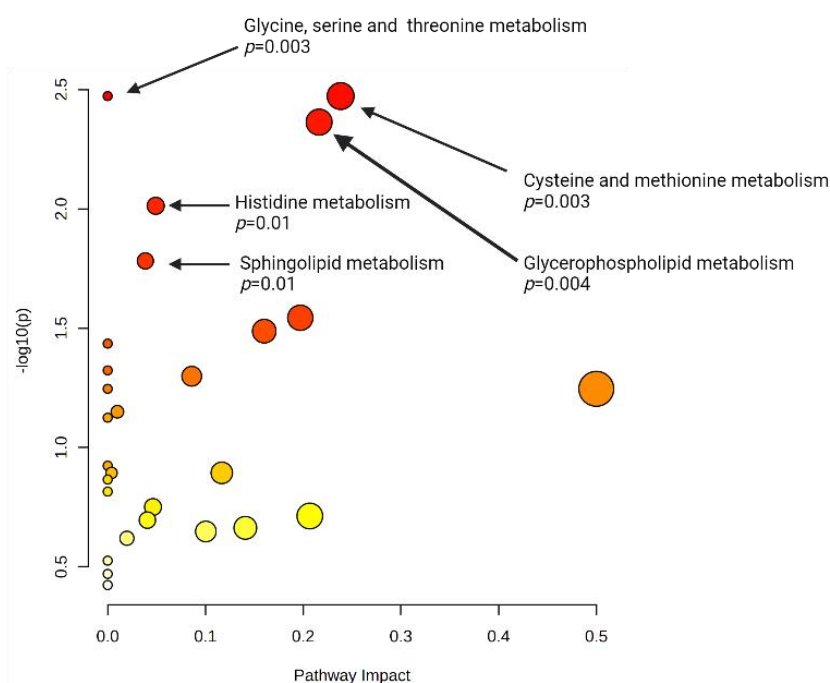
Dysregulated pathways	
Cysteine and methionine metabolism	Valine, leucine and isoleucine biosynthesis
Glycine, serine and threonine metabolism	alpha-Linolenic acid metabolism
Glycerophospholipid metabolism	Glycosylphosphatidylinositol (GPI)-anchor biosynthesis
Histidine metabolism	Arginine biosynthesis
Sphingolipid metabolism	Butanoate metabolism
Alanine, aspartate and glutamate metabolism	Retinol metabolism
Porphyrin and chlorophyll metabolism	Citrate cycle (TCA cycle)
Glyoxylate and dicarboxylate metabolism	Pyruvate metabolism
Linoleic acid metabolism	Propanoate metabolism
Arginine and proline metabolism	Lysine degradation
Nitrogen metabolism	Glycolysis / Gluconeogenesis
D-Glutamine and D-glutamate metabolism	Glutathione metabolism
Primary bile acid biosynthesis	Arachidonic acid metabolism
Tyrosine metabolism	Aminoacyl-tRNA biosynthesis

Figure 12 | Overview of pathway analysis and identified pathways of interest

The top five dysregulated pathways are annotated and include;

- Cysteine and methionine metabolism

- Glycerophospholipid metabolism

- Sphingolipid metabolism

- Histidine metabolism

- Glycine, serine and threonine metabolism

The network plots for most relevant are provided in Appendix 4. A heatmap of the 28 identified pathways and which biomarkers were found to be involved in ≥ 1 of the pathways is displayed in Figure 13. Out of the 92 candidate biomarkers 29 featured across the 28 identified pathways. There are four metabolites that make multiple appearances across the 28 pathways and include: alpha-ketobutyrate, cystathionine, glutamate and pyruvate.
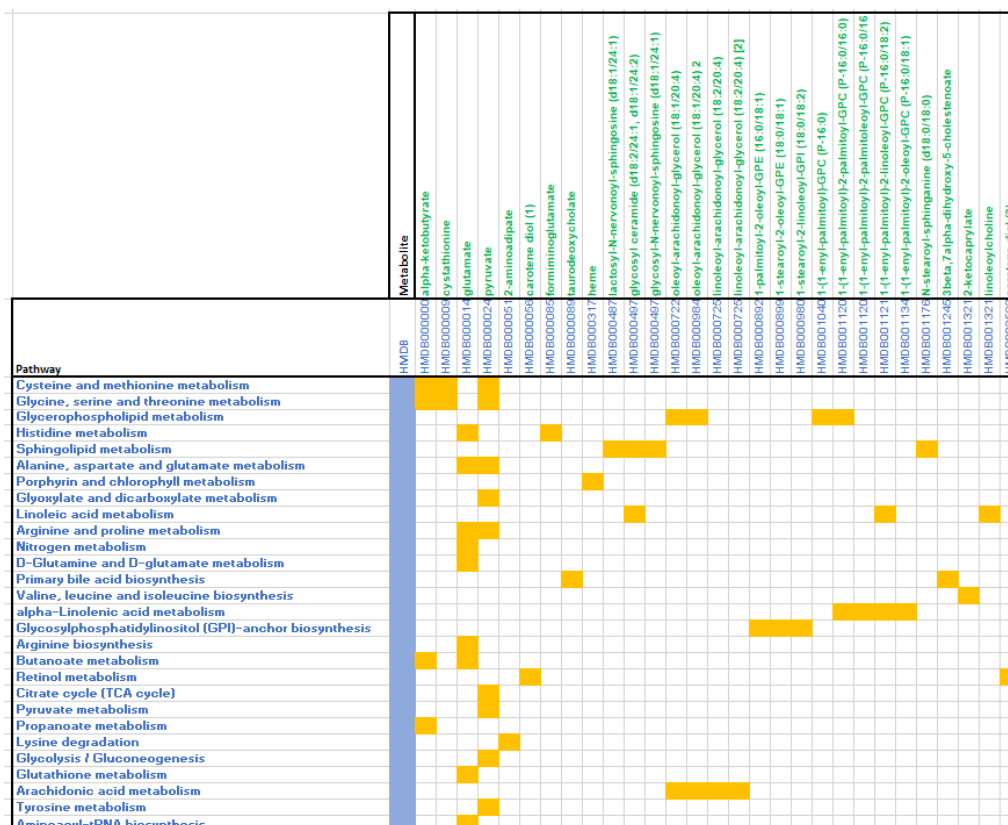
Figure 13 | Heatmap displaying biomarkers with ≥ 1 feature across identified metabolic pathways

4.1.4 Correlation analysis

To further refine the candidate biomarkers down from 92,b only those that were related to the outcomes of interest were taken forwards. For each outcome of interest (eight CMR variables and peak VO$_2$) a correlation plot was created and selected to report *ONLY* the top 20 correlates for the given outcome which met statistical significance ($p<0.05$). An example is provided in Figure 14. This plot shows the top twenty correlates with LV mass to volume ratio of which 17 are metabolites. All 17 demonstrate moderate-to-good relationship (r=0.42 – 0.49). Two of the CMR variables (LV mass indexed to BSA and LV GLS) did not have any significant correlations with any of the candidate biomarkers and were subsequently removed from further analysis. Forty-eight biomarkers were identified that had significant correlations with the seven outcomes of interest which can be visualised in the correlation pie-chart plots in Figure 15.
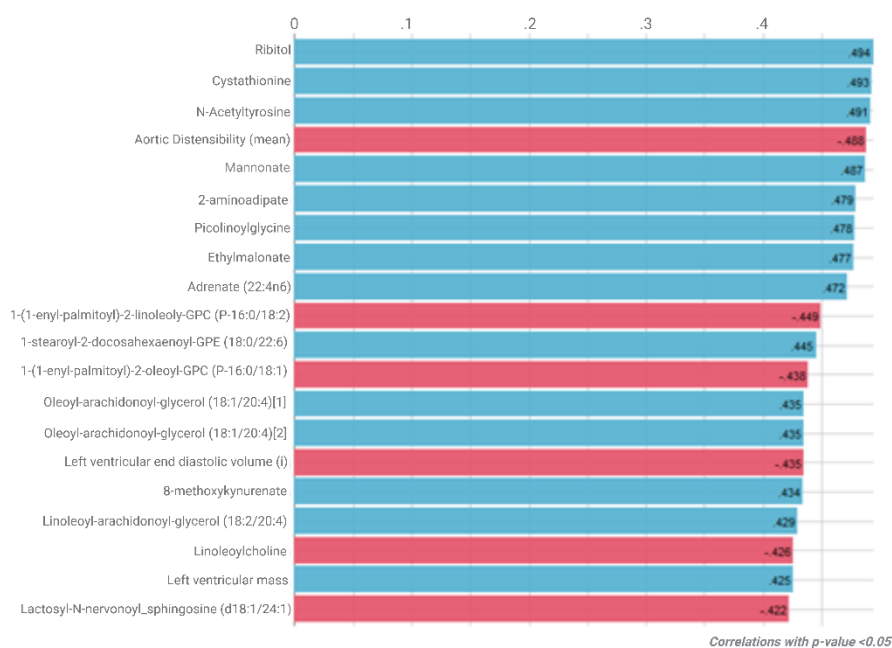
Figure 14 | Plot of top 20 correlates with LV mass:volume ratio with p<0.05 (output from MetaboAnalyst)

Correlated variable is provided on the y-axis. X axis = correlation co-efficient. Blue bars = positive correlation and red bars = negative correlation.
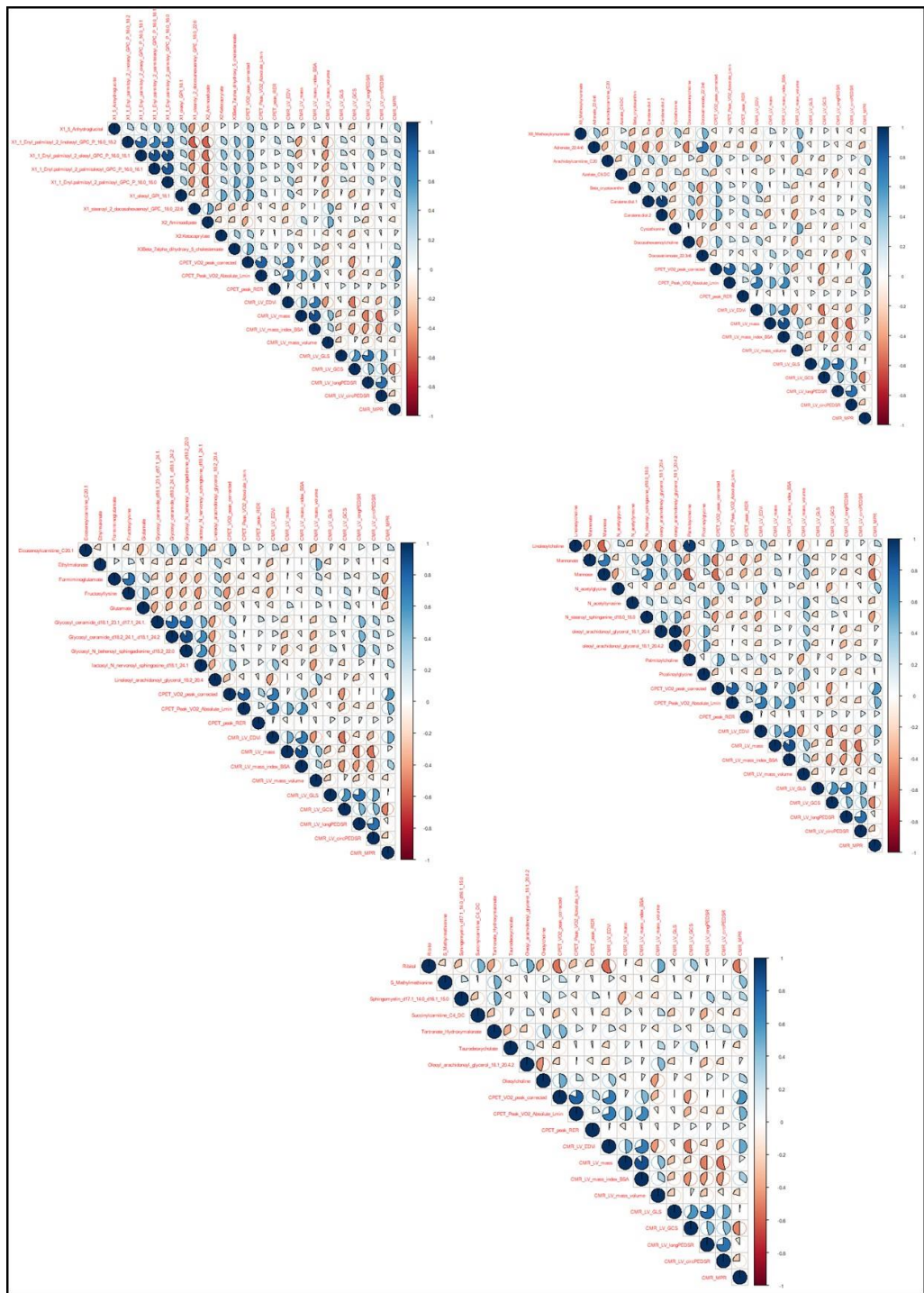
Figure 15 | Correlograms with pie-plots between seven outcomes and 48 candidate biomarkers

Across the correlograms twelve biomarkers were significantly related to LV EDVi (measure associated with diastole), 18 to LV mass:volume ratio (measure of concentric remodelling), 12 to longitudinal PEDSR (measure of diastolic function), four to circumferential PEDSR (another measure of diastolic

function), 14 to MPR (measure of microvascular function) and 16 to peak VO$_2$ (measure of exercise capacity) which can be visualised in Figure 16.

Biomarker/Outcome	LV_EDVi	LV_M:V	L_PEDSR	C_PEDSR	GCS	MPR	PeakVO2
1,5-Anhydroglucitol (1,5-AG)						0.348	
1-(1-enyl-palmitoyl)-2-linoleoyl-GPC (P-16:0/18:2)		-0.449	0.375				0.508
1-(1-enyl-palmitoyl)-2-oleoyl-GPC (P-16:0/18:1)		-0.438	0.386				0.479
1-(1-enyl-palmitoyl)-2-palmitoleoyl-GPC (P-16:0/16:1)	0.373		0.320				
1-(1-enyl-palmitoyl)-2-palmitoyl-GPC (P-16:0/16:0)						0.411	0.540
1-oleoyl-GPI (18:1)					-0.329		0.539
1-Stearoyl-2-docosahexaenoyl-GPE (18:0/22:6)			0.445				
2-Aminoadipate		0.479					
2-Ketocaprylate					-0.302		
3-Beta,7-alpha-dihydroxy-5-cholestenoate	0.390						0.527
8-Methoxykynurenate		0.434					
Adrenate (22:4n6)	-0.407	0.472					
Arachidoylcarnitine (C20)						0.397	
Azelate (C9-DC)			-0.036				
Beta-cryptoxanthin	0.442					0.346	0.475
Carotene diol (1)						0.393	0.491
Carotene diol (2)							0.494
Cystathionine		0.493					
Docosahexaenoylcholine							0.469
Docosatrienoate (22:3n6)			-0.317	-0.422			
Eicosenoylcarnitine (C20:1)							0.469
Ethylmalonate		0.477					
Formiminoglutamate						-0.398	
Fructosyllysine	-0.383				0.302	-0.475	
Glutamate					0.282		
Glycosyl ceramide (d18:1/23:1, d17:1/24:1)			0.453	0.349			
Glycosyl ceramide (d18:2/24:1, d18:1/24:2)			0.454	0.310			
Glycosyl-N-behenoyl-sphingadienine (d18:2/22:0)			0.500	0.364			
Lactosyl-N-nervonoyl-sphingosine (d18:1/24:1)	0.408	-0.422					
Linoleoyl-arachidonoyl-glycerol (18:2/20:4)	-0.427	0.429					
Linoleoylcholine		-0.426					0.530
Mannonate		0.487				-0.438	-0.497
Mannose						-0.525	-0.552
N-acetylglycine	0.428				-0.368	0.396	
N-acetyltyrosine		0.491					
N-stearoyl-sphinganine (d18:0/18:0)	-0.382					-0.412	
Oleoyl-arachidonoyl-glycerol (18:1/20:4)		0.435		-0.329			
Oleoyl-arachidonoyl-glycerol (18:1/20:4) [2]		0.435		-0.329			
Palmitoylcholine	0.377						0.517
Picolinoylglycine		0.478					
Ribitol	-0.558	0.494			0.373	-0.525	-0.548
S-methylmethionine						0.416	
Sphingomyelin (d17:1/14:0, d16:1/15:0)			0.352				
Succinylcarnitine (C4-DC)			-0.362				
Tartronate (hydroxymalonate)						0.412	
Taurodeoxycholate						0.343	
Oleoyl-arachidonoyl-glycerol (18:1/20:4) [2]		0.435					
Oleoylcholine	0.398						0.498

Figure 16 | Correlation heat map

Heat map representing the biomarkers that featured in the top 20 significant correlates *per* outcome of interest. Blue indicates a positive relationship and red a negative one.

Across the 48 candidate biomarkers and the heatmap we can see that lipid species feature quite heavily e.g.; 1-(1-enyl-palmitoyl)-2-linoleoyl-GPC with particular representation from those in the ceramide/sphingolipid pathways and carnitines (highlighted with the red outlines).

4.2 Pre-, post-analysis

In this dataset there were 48 samples (24 paired samples) by 845 compounds. Two features were identified with constant/single value missing across the sample IDs and were subsequently removed. 3359 (8.3%) was identified as missing data and were imputed by 1/5 minimum positive value of the corresponding variable. Data were then normalised by sum, log10 transformed with data standardised across the dataset Appendix 2.

Twenty-four cases completed the MRP intervention and had plasma for metabolomic analysis. There were significant cardio-metabolic improvements including weight loss (13.6Kg), blood pressure (13mmHg systolic), reduced arterial stiffness, reduced concentric remodelling and insulin resistance (Table 5). Furthermore, there was a significant improvement in glycaemic control with a clinically meaningful reduction in fasting glucose (-1.9mmol) and 20 (83%) participants achieving normoglycaemia by 12 weeks

Table 5 | Pre-, post-MRP change in clinical characteristics

Variable	Pre-MRP N=24	Post-MRP N=24	*P* value
Clinical characteristics			
Weight (kg)	106.7 ± 16.2	93.0 ± 15.0	**<0.001**
BMI (kg/m2)	37.4 ± 5.9	32.6 ± 5.65	**<0.001**
Systolic BP (mmHg)	145.9 ± 15.9	133 ± 18.0	**0.005**
Diastolic BP (mmHg)	91.1 ± 7.4	86.5 ± 9.06	0.058
Heart rate (bpm)	73.1 ± 8.6	67.8 ± 9.77	**0.003**
HbA1c (%)	7.2 ± 1.1	6.2 ± 0.7	**<0.001**
HbA1c (mmol/mol)	54.8 ± 11.9	44.4 ± 7.6	**<0.001**
HOMA-IR	12.2 ± 8.2	4.79 ± 2.36	**<0.001**
Cardiovascular Imaging			
LV Massi (g/m)	0.77 (0.14)	0.74 ± 0.14	0.059
LV EDVi (mL/m)	69.9 ± 11.3	75.6 ± 14.2	**0.001**
LV mass:volume (g/mL)	0.84 ± 0.13	0.80 ± 0.11	**0.017**
LV EF (%)	70.0 ± 7.4	65.2 ± 6.09	**0.001**
LV GLS (%)	16.6 ± 2.8	16.0 ± 1.84	0.021
LV GCS (%)	21.0 ± 2.3	19.6 ± 2.18	**0.039**
LV LongPEDSR (s-1)	0.79 ± 0.15	0.73 ± 0.14	**<0.001**
LV CircPEDSR (s-1)	1.00 ± 0.20	0.96 ± 0.23	<0.001
Mean Ao Distens (mmHg^{-1}x10^{-3})	3.7 ± 1.9	4.56 ± 2.26	**<0.001**
MPR	3.0 ± 1.0	3.15 ± 0.89	**0.310**
Cardiopulmonary exercise testing			
Peak VO2 (mL/kg/min)	16.4 ± 4.47	18.3 ± 5.51	**<0.001**

Abbreviations: BMI = body mass index, LV EF = Left ventricular ejection fraction, LV Massi = Left Ventricular Mass Indexed to height, mass:volume = mass to volume ratio , LV EDVi = Left Ventricular End Diastolic Volume indexed for height, GLS = global longitudinal strain, LongPEDSR = Longitudinal Peak Early Diastolic Strain rate, CircPEDSR = Circumferential Peak Early Diastolic Strain Rate, GCS = global circumferential strain, Mean Ao Distens = Mean aortic distensibility, MPR= Myocardial perfusion reserve. Data are reported as mean ± standard deviation, count (percent) or median (interquartile range). Bold font highlights statistically significant difference with significance level of 95%.
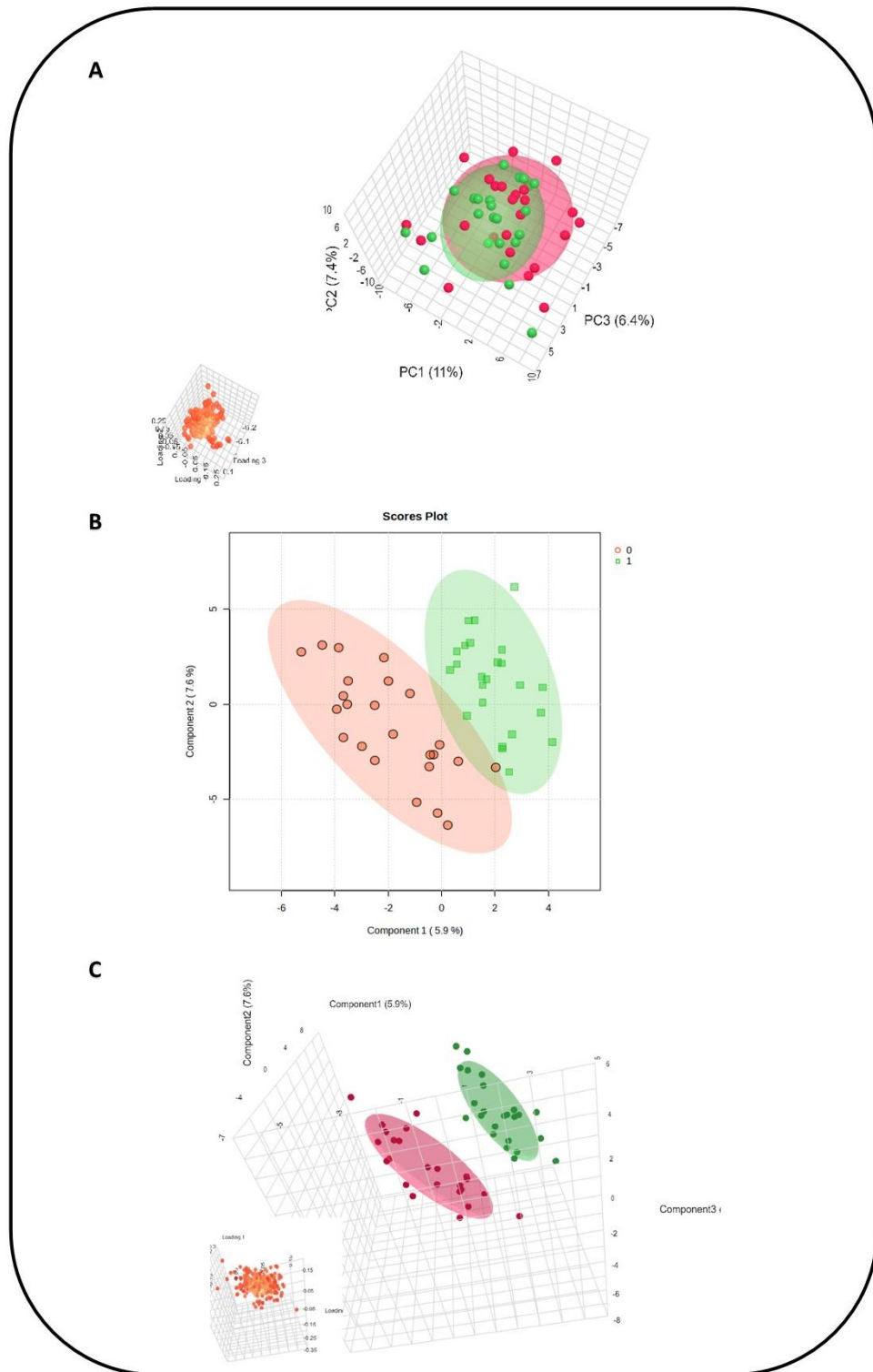
Figure 17 | Principal component and partial least squares discriminant analysis plots for pre-, and post plasma metabolites (Outputs from MetaboAnalyst)

Plot A: 3D Principal component analysis plot with the first three principal components collectively accounting for 24.8% of the variation within the dataset. Plot B: 2D partial least squares discriminant plot with first two

predictive components and Plot C: 3D partial least squares discriminant plot with first three predictive components.

The three-dimensional PCA score plot based on the plasma levels of identified metabolites at baseline and post-MRP is displayed in Figure 17A. In this plot there appears to be some separation but also overlap i.e.; partial discrimination between the two time-points based on these metabolites. However, we get better differentiation of the two groups, due to variation in their metabolic profiles, from both the two-dimensional PLS-DA score plot with predictive component 1 and component 2 better and the three- two-dimensional PLS-DA score plot (Figure 17B-C) this is potentially due to the difference in the methods i.e.; PCA is an unsupervised vs. PLS-DA which is supervised method of descriptive modelling. The Q^2 value for 2 and 3 components were low at 0.16 and 0.10, respectively. However, the corresponding R^2 values were good at 0.81 and 0.90, respectively, together indicating moderate predictive power of the model. The empirical p value for the permutation test was $p = 0.85$ for 100 permutations and $p = 0.84$ for 2000 permutations indicating that the null hypothesis cannot be rejected and suggests poor separation/differences across the metabolome between the two groups.

A hierarchical clustering heatmap of the dataset is shown in Figure 18 below. This visualisation indicates no evidence of a systematic change to the metabolome between the two time-points and largely appear to be paired i.e.; class 0 almost alternating with class 1. This is as one would expect for a given dietary intervention, that is, we would not expect the entire metabolome to be affected by a simple 12-week MRP. Further, the horizontal lines correspond to each metabolite and the vertical to the timepoint with some, upon close inspection, appearing to differ between the two time-points (classes) which may represent those metabolites that are discriminating between the timepoints in the previous PCA and PLS-DA.
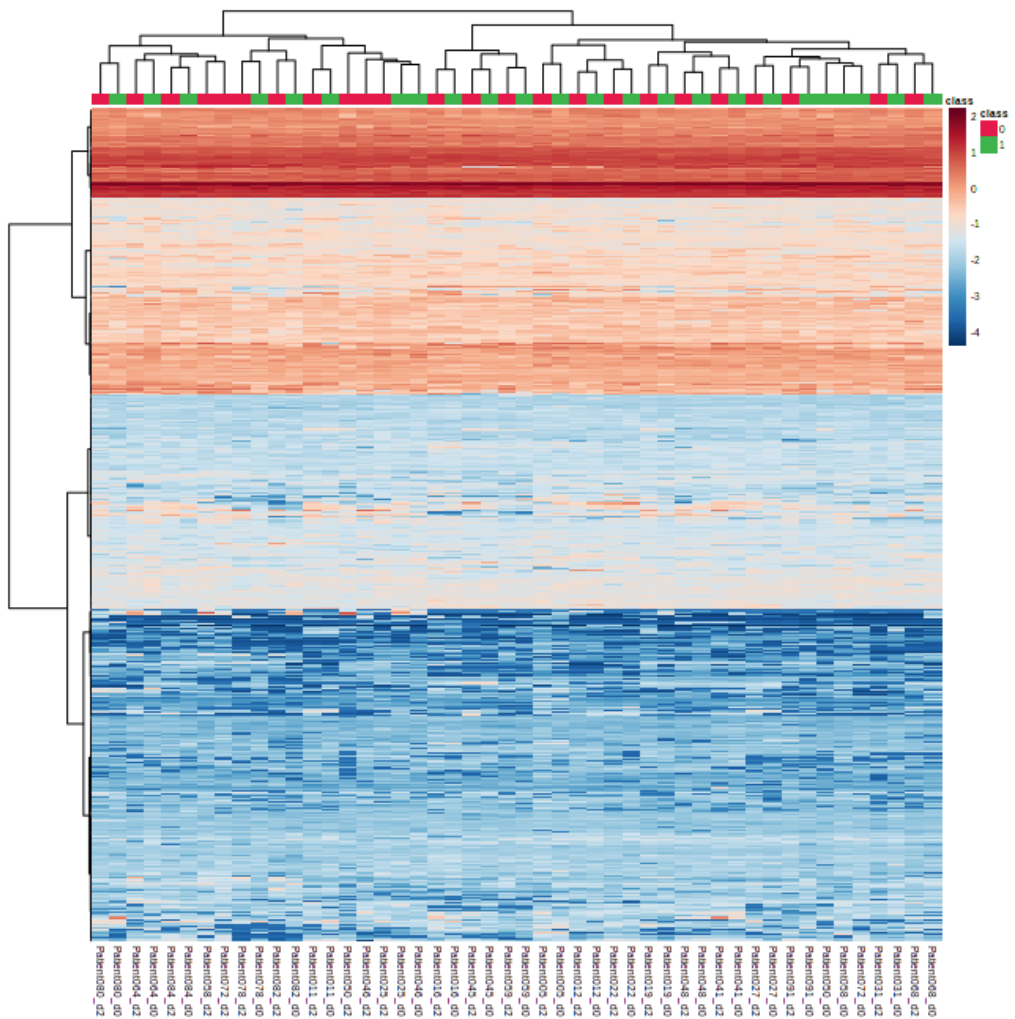
Figure 18 | Hierarchical clustering heatmap pre-, post-MRP plasma metabolome

There was a FC identified between cases-controls in a total of 123 metabolites (60 downregulated and 63 upregulated see Figure 19). Of these a total of 47 had a FC 1.5 with adjustment for FDR meeting the threshold for statistical significance (p<0.05) as presented in Figure 20.
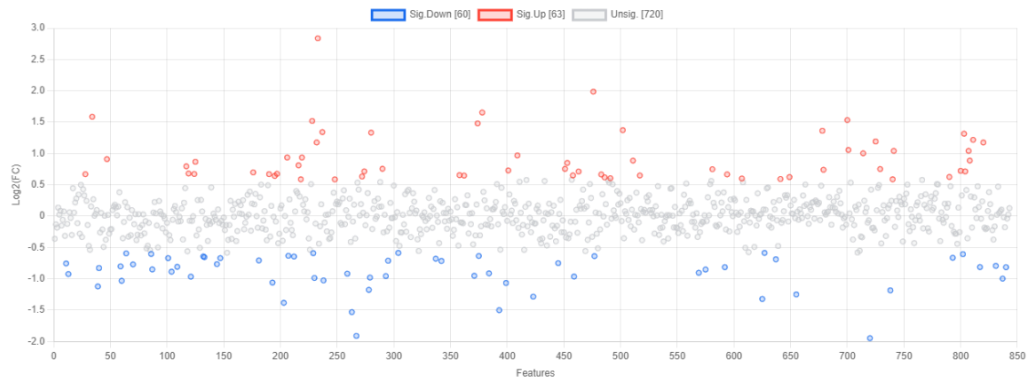
Figure 19 | Scatter plot for fold-change between pre-, and post-MRP across 847 metabolites (outputs from MetaboAnalyst)

For both plots each circle represents a metabolite with those coloured blue = significantly downregulated in cases *vs*. control, red = significantly up regulated in cases *vs*. control and grey = no significant fold change between cases and control
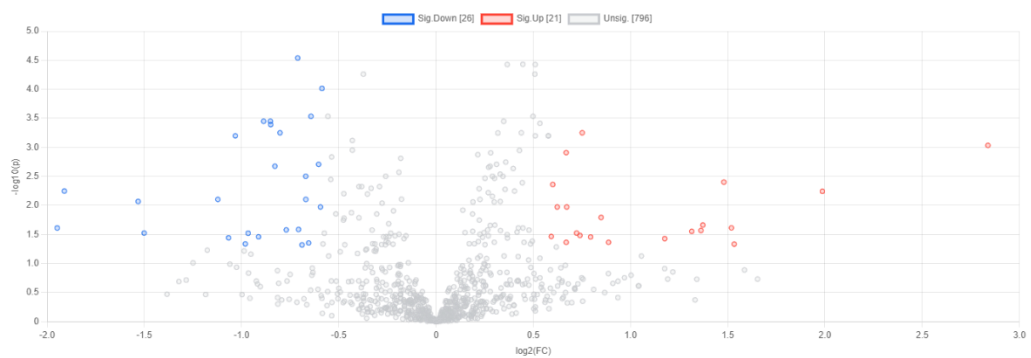
Figure 20 | Volcano plot identifying biomarkers with a significant fold-change and adjusted FDR (outputs from MetaboAnalyst)

When this list of 47 candidate biomarkers were cross-referenced with the 48 biomarkers identified in the case-control analysis there were 11 biomarkers that matched across the two analyses Table 6.

Table 6 | Description of candidate biomarkers

Metabolite/candidate biomarker	HMDB	Super pathway	Sub-pathway	Structure
N-acetylglycine	HMDB00532	Amino Acid	Glycine, Serine and Threonine Metabolism	
1-carboxyethylvaline	HMDB0240627	Amino Acid	Leucine, Isoleucine and Valine Metabolism	
1-carboxyethylphenylalanine	HMDB0240628	Amino Acid	Phenylalanine Metabolism	
Deoxycholic acid (12 or 24)-sulfate	HMDB0000626	Lipid	Secondary Bile Acid Metabolism	*Minus the sulphate group at position 12 or 24
N-stearoyl-sphinganine	HMDB0011761	Lipid	Dihydroceramides	
1-stearoyl-2-oleoyl-GPE	HMDB08993	Lipid	Phosphatidylethanolamine (PE)	
1-(1-enyl-palmitoyl)-GPC	HMDB10407	Lipid	Lysoplasmalogen	
Hydroxybutyroylglycine	HMDB0094716	Lipid	Fatty Acid Metabolism (Acyl Glycine)	
Heme	HMDB03178	Cofactors and Vitamins	Hemoglobin and Porphyrin Metabolism	
Dihydroferulic acid sulfate	HMDB41724	Xenobiotics	Food Component/Plant	
Tartronate (hydroxymalonate)	HMDB35227	Xenobiotics	Food Component/Plant	
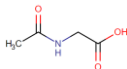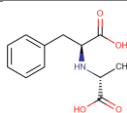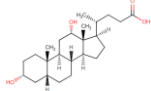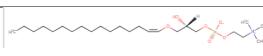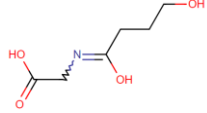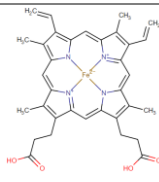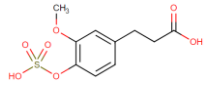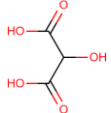
This table provides the compound name, HMDB ID, super and sub-pathways and the chemical structure. The chemical structures have been taken from the HMDB (https://hmdb.ca/).

Three biomarkers are involved in amino acid metabolism, five lipid metabolism, one co-factor (heme) and the remaining two are identified as xenobiotics. Xenobiotics are compounds that are extrinsic to the normal human metabolism. The difference in metabolite concentration across the three groups and associated *p*-values are provided per metabolite/candidate biomarker in Figure 21 and Figure 22. Across all 11 biomarkers the post-MRP plasma levels appear to move toward the HC levels, except for N-Stearoyl-Sphinganine, which across the plots does not appear to change.
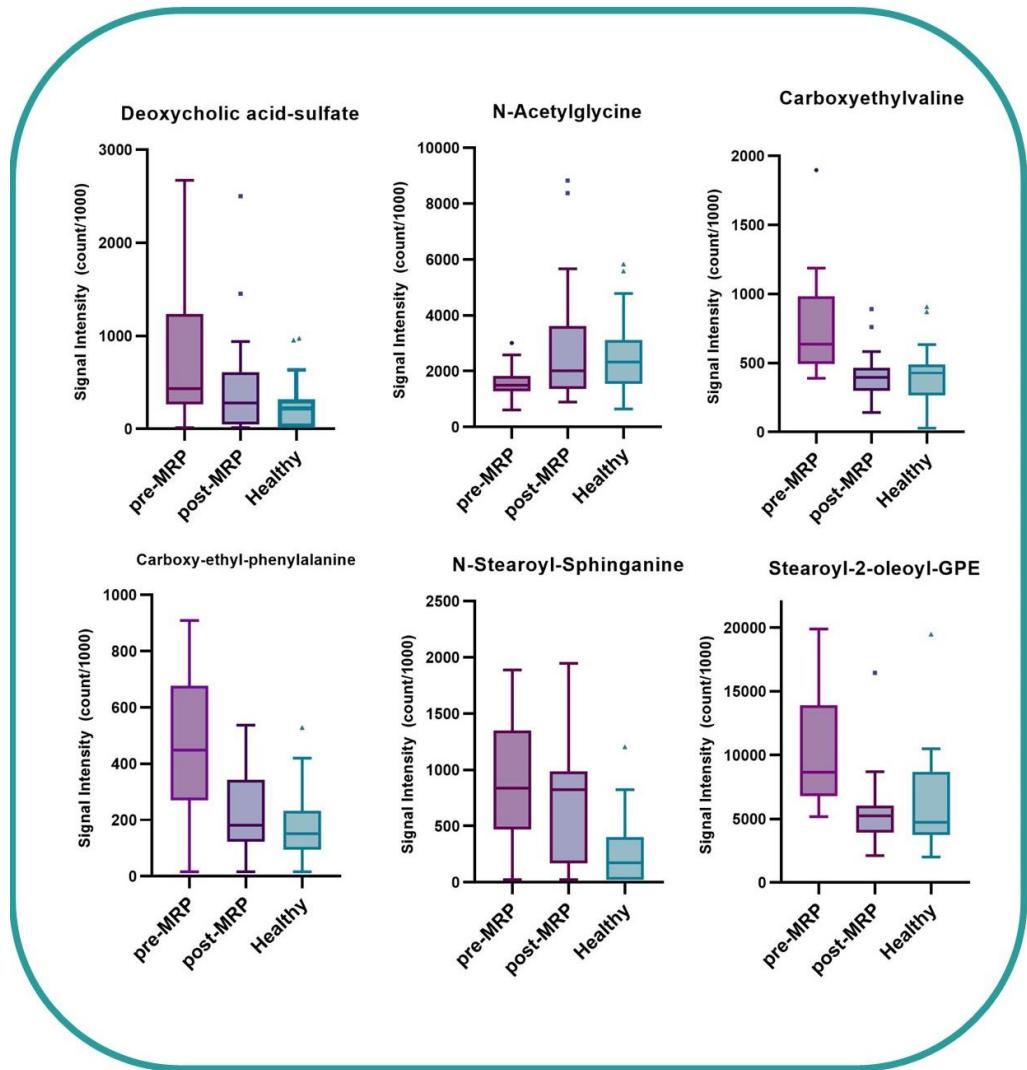
Figure 21 | Box and whisker plots for candidate biomarker levels pre-MRP, post-MRP and healthy
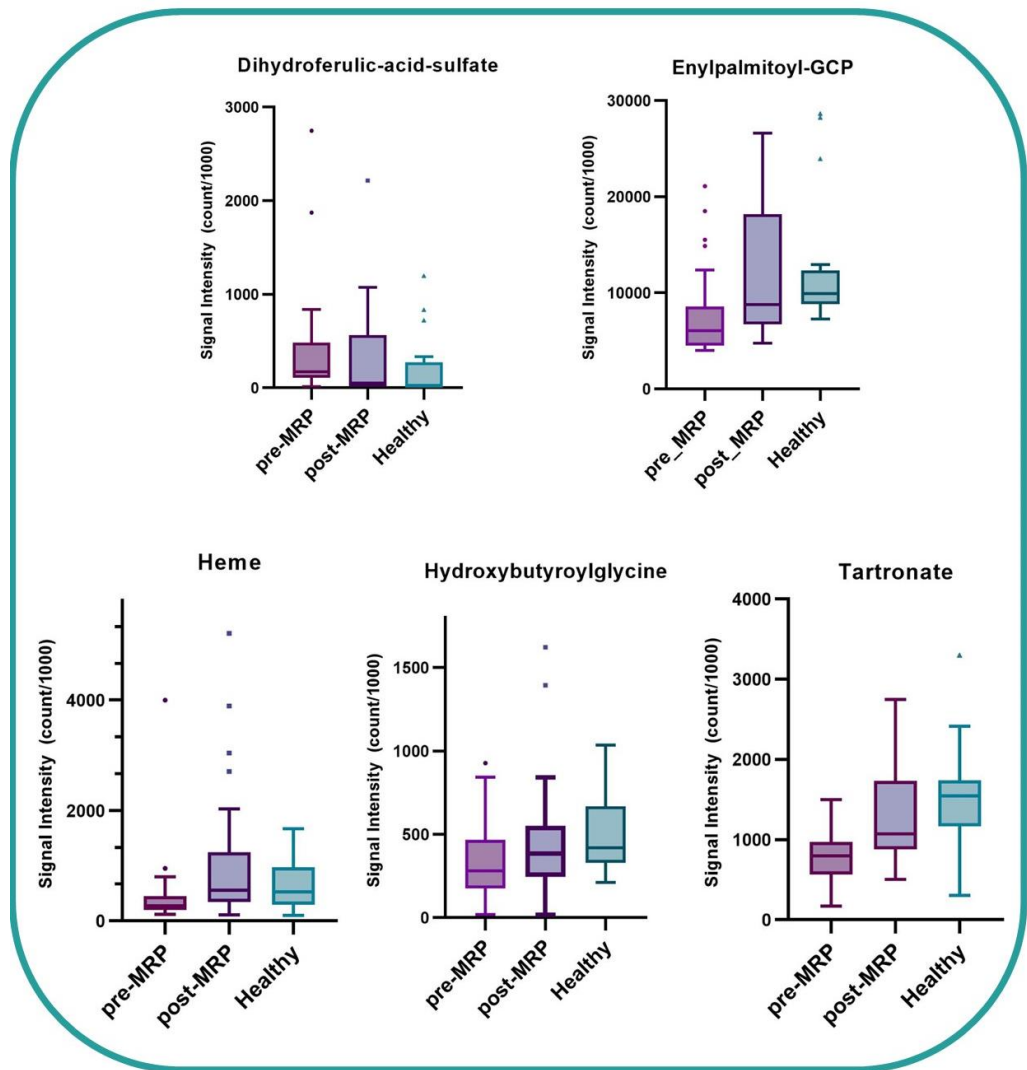
Figure 22 | Continuation of box and whisker plots of plasma levels of candidate biomarkers by group

The relationship between change in the candidate biomarkers and change cardiovascular outcomes of interest are presented in the correlation plot below in Figure 23. This is followed by the correlation plot for the relationship between change in the candidate biomarkers and key cardiometabolic indices in Figure 24.

	c_Stearoyl_2_oleoyl_GPE	c_Carboxyethylphenylalanine	c_Carboxyethylvaline	c_Tartronate	c_LV_EDVi	c_Enylpalmitoyl_GPC	c_Dihydroferulic_acid_sulfate	c_heme	c_N_Stearoyl_Sphinganine	c_Hydroxybutyroylglycine	c_N_Acetylglycine	c_LV_mass_volume	c_MPR	c_LV_longPEDSR	c_CPET_VO2	c_LV_GCS	c_LV_circPEDSR
c_Deoxycholic.acid_sulfate	0.3	0.17	0.32	-0.14	0.1	-0.02	-0.11	-0.11	0.19	0.06	0.19	-0.02	0.24	-0.47	-0.09	0.09	-0.03
c_Stearoyl_2_oleoyl_GPE		0.32	0.52	-0.14	0.21	-0.08	0.07	-0.24	-0.02	-0.51	-0.42	-0.23	-0.12	0.17	-0.22	-0.19	-0.1
c_Carboxyethylphenylalanine			0.74	0.13	0.19	0.13	0.02	0.15	0.12	-0.1	-0.06	-0.07	-0.06	0.16	-0.29	-0.2	0.06
c_Carboxyethylvaline				0.13	0.23	0	0.06	-0.07	0.08	-0.09	-0.11	-0.05	-0.01	0.13	-0.37	-0.32	0.02
c_Tartronate					0.52	0.52	-0.1	-0.02	-0.3	-0.11	-0.34	0.11	0.23	-0.11	0.35	-0.39	-0.04
c_LV_EDVi						0.15	-0.06	0.05	-0.18	-0.42	-0.29	-0.4	-0.13	0.15	0.19	-0.1	0.31
c_Enylpalmitoyl_GPC							0.4	0.33	0.14	0.16	-0.18	0.1	0.15	-0.2	0.09	-0.34	-0.2
c_Dihydroferulic_acid_sulfate								0.57	-0.06	-0.2	-0.32	0.02	-0.37	0.05	-0.26	-0.05	-0.02
c_heme									-0.08	-0.02	0.02	-0.21	-0.38	0.03	0.13	0.25	0.28
c_N_Stearoyl_Sphinganine										0.55	0.59	0.2	0.08	-0.15	-0.17	-0.08	-0.18
c_Hydroxybutyroylglycine											0.63	0.19	0.14	-0.21	0.17	0.04	-0.04
c_N_Acetylglycine												0.06	0.23	-0.15	0.03	0.08	-0.16
c_LV_mass_volume													0.42	-0.25	-0.33	-0.37	-0.42
c_MPR														-0.26	-0.06	-0.33	-0.36
c_LV_longPEDSR															-0.07	0.12	0.11
c_CPET_VO2																0.19	0.24
c_LV_GCS																	0.69

Figure 23 | Correlogram of change in candidate biomarkers and change in CMR outcomes of interest

The larger the circle the stronger the relationship. All non-significant relationships have a blank grid. The colour of the circle represents the direction of the relationship and strength with the correlation co-efficient printed within the grid.

Across the eleven candidate biomarkers there were a number of weak correlations with outcomes of interest; the change in tartronate was positively related to the change LV EDVi (r= 0.52) and negatively related to the change LV GCS (r=-0.39), change in carboxyethylvaline was negatively related to the change in VO2max (r=-0.37) and LV GCS (r=-0.32), change in dihydroferulic acid sulphate and heme were negatively related to change in MPR (r=-0.37 and -0.38, respectively), change in deoxycholic acid sulphate was negatively related

to the change in longitudinal LV PEDSR (r=-0.47) and enylpalmitoyl-GCP was negatively related to change in LV GCS (r=-0.34).

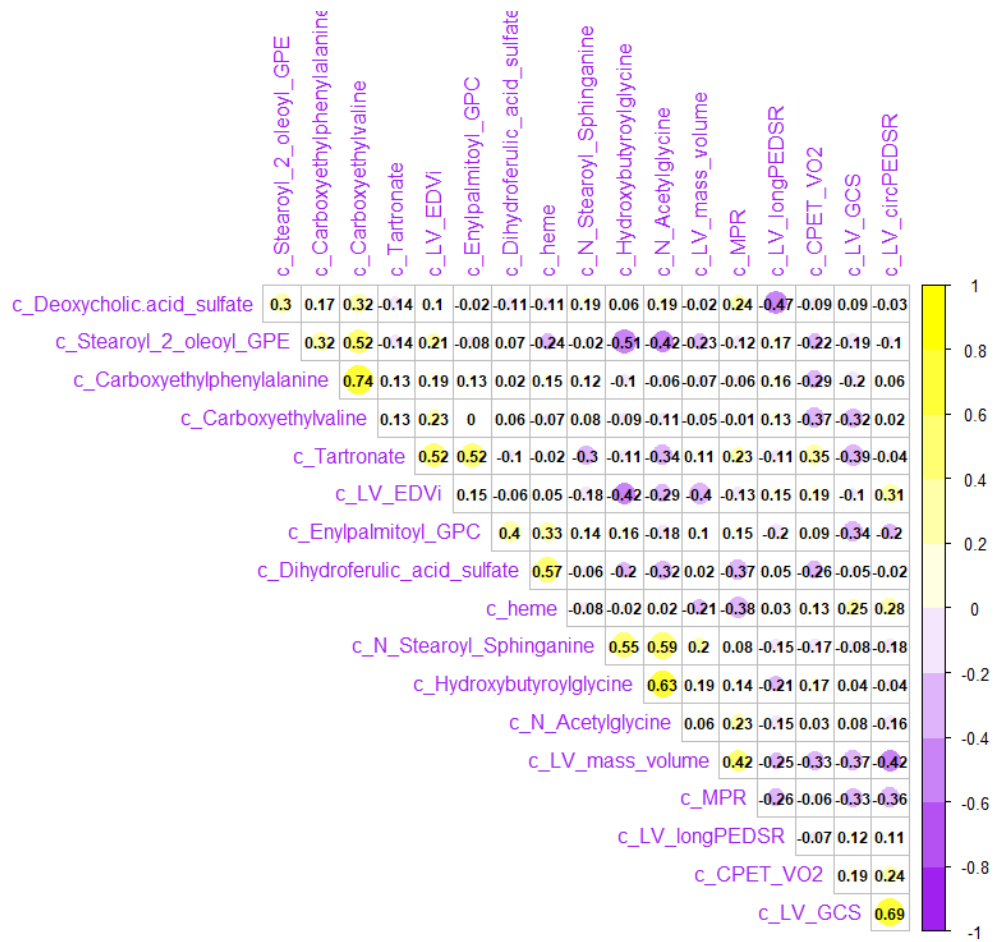|	c_N_Acetylglycine	c_Deoxycholic.acid_sulfate	c_N_Stearoyl_Sphinganine	c_HbA1c	c_weight_kg	c_Carboxyethylphenylalanine	c_Carboxyethylvaline	c_Stearoyl_2_oleoyl_GPE	c_glucose	c_HOMA_IR	c_Dihydroferulic_acid_sulfate	c_heme	c_cholesterol	c_Enylpalmitoyl_GPC	c_Tartronate
c_Hydroxybutyroylglycine	0.63	0.06	0.55	0.04	-0.51	-0.1	-0.09	-0.51	-0.14	-0.23	-0.2	-0.02	0.03	0.16	-0.11
c_N_Acetylglycine		0.19	0.59	0.1	-0.3	-0.06	-0.11	-0.42	0.09	-0.12	-0.32	0.02	0.05	-0.18	-0.34
c_Deoxycholic.acid_sulfate			0.19	0.25	-0.29	0.17	0.32	0.3	0.39	0.05	-0.11	-0.11	0.1	-0.02	-0.14
c_N_Stearoyl_Sphinganine				0.61	-0.22	0.12	0.08	-0.02	0.36	0.05	-0.06	-0.08	-0.06	0.14	-0.3
c_HbA1c					-0.13	0.55	0.48	0.35	0.62	0.2	0.11	0.2	-0.26	0.16	-0.13
c_weight_kg						0.06	0.06	0.31	0.14	0.35	0.31	-0.17	0.02	-0.3	-0.29
c_Carboxyethylphenylalanine							0.74	0.32	0.65	0.52	0.02	0.15	-0.21	0.13	0.13
c_Carboxyethylvaline								0.52	0.56	0.3	0.06	-0.07	-0.24	0	0.13
c_Stearoyl_2_oleoyl_GPE									0.37	0.36	0.07	-0.24	-0.22	-0.08	-0.14
c_glucose										0.77	0.08	0.14	0.07	-0.05	-0.12
c_HOMA_IR											0.04	0.07	0.18	-0.12	-0.03
c_Dihydroferulic_acid_sulfate												0.57	-0.06	0.4	-0.1
c_heme													0.09	0.33	-0.02
c_cholesterol														0.23	0.25
c_Enylpalmitoyl_GPC															0.52

Figure 24 | Correlogram of change in candidate biomarkers and change in key cardiometabolic indices

The larger the circle the stronger the relationship. All non-significant relationships have a blank grid. The colour of the circle represents the direction of the relationship and strength with the correlation co-efficient printed within the grid.

The plot above indicates that there are stronger relationships between the change in candidate biomarkers and key cardiometabolic indices, namely glycaemic control, as compared to those observed for the outcomes of interest. Firstly, change in weight was moderately related to a change in hydroxybutyroylglycine (r=-0.51). Change in HbA1c was moderately related to a change in circulating carboxyethylphenylalanine (r=0.55), change in stearoyl-sphinganine (r=0.61) and change in carboxyethylvaline (r=0.48). Change in

fasting glucose demonstrates a good relationship with change in carboxyethylphenylalanine (r=0.65) and change in carboxyethylvaline (r=0.56). Change in HOMA-IR was also related to change in carboxyethylphenylalanine (r=0.55) and change in carboxyethylvaline (r=0.48). The alterations observed in amino acid and lipid metabolism are potentially related to changes in glycaemic control following the MRP. The scatter plots below in Figure 25 show the linear relationship between the three strongest correlations; change in weight and change in hydroxybutyroylglycine (negatively correlated), change in HbA1c and change in stearoyl-sphinganine (positively correlated) and between change in fasting glucose and change in carboxyethylphenylalanine (positively correlated).

Figure 25| Scatter plots for strongest relationships between biomarkers and glycaemic indices
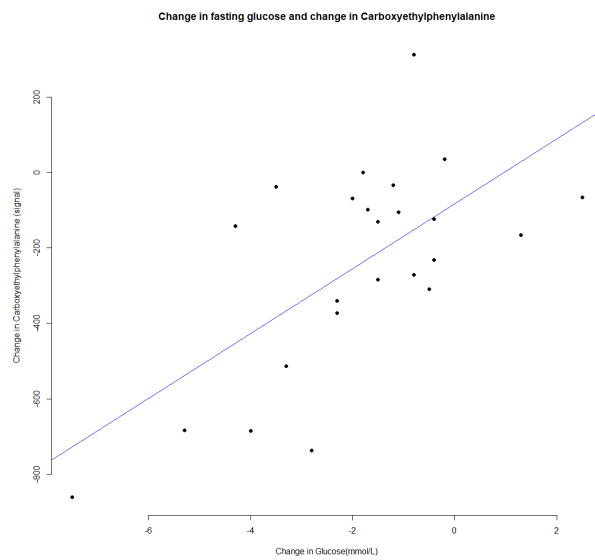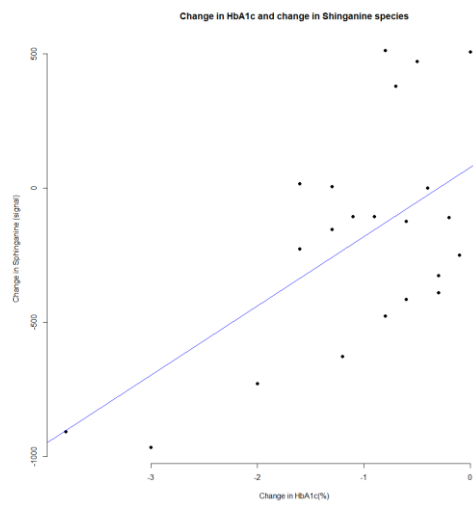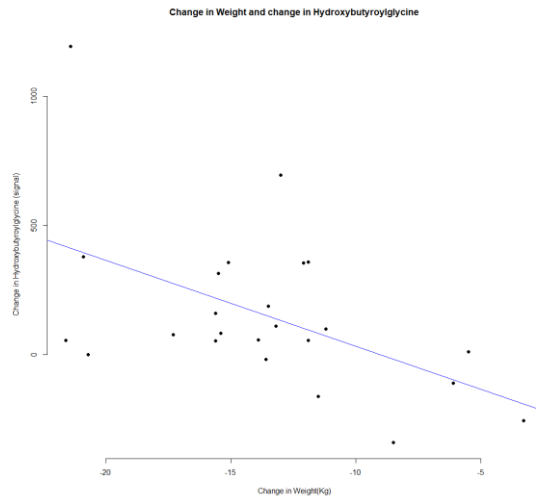
5. Discussion

This project aimed to identify and describe the metabolic signature in people with stage A/B HF and response to low-calorie diet. The key findings include the identification of a differential metabolic signature in people with stage A/B HF to their healthy counterparts which translates to the dysregulation of specific metabolic pathways. Following the MRP, some 48 metabolites were differentially expressed of which 11 mapped to the first analysis (case-control). The circulating plasma levels of these 11 metabolites demonstrated a marked shift towards the healthy control levels. Finally, the change in three metabolites were significantly related to the change in key metabolic indices following the MRP. However, from these data no convincing relationship between the candidate biomarkers and measures of cardiovascular reverse remodelling were observed. The improvement in cardiovascular structure and function observed in these patients, post MRP, is likely related to the improved cardiometabolic status, namely glycaemic control and weight.

5.1 Case-Control

5.1.1 Metabolic Signature

The first objective of this study was to determine if the metabolic signature differs between people with stage A/B HF and matched healthy controls employing an untargeted metabolomic approach. The two groups can be discriminated by the variation in their metabolic profiles, as is elegantly demonstrated in the data visualisations, with both PCA and PLS-DA for this case-control analysis. This is further supported by the differential expression of ninety-four metabolites. The metabolic signature, in the stage A/B HF cohort, is characterised by impaired lipid and amino-acid metabolism with some perturbations in carbohydrate metabolism. These data are in-line with a recent systematic review and meta-analysis of cross-sectional and prospective metabolomic studies evaluating potential association(s) with plasma profiles and pre-diabetes and/or T2D (56). Across the 46 studies lipids (namely; phospholipids, sphingomyelins, and triglycerides), and amino acids (namely; branched-chain amino acids, aromatic amino acids, glycine, and glutamine), were significantly higher in those with either pre-diabetes or T2D. The top

three upregulated metabolites identified in this study were; 1-(1-enyl-palmitoyl)-2-palmitoyl-GPC (P-16:0/16:0), 1-(1-enyl-palmitoyl)-2-linoleoyl-GPC (P-16:0/18:2) and 1-(1-enyl-palmitoyl)-2-palmitoyl-GPC (P-16:0/16:0) all of which are glycerophospholipids, and more specifically glycerophosphocholines, which are lipids containing a glycerol moiety carrying a phosphocholine at the 3rdposition. Their properties include lipid membrane homeostasis, mitochondrial NAD+/NADH metabolism and skeletal muscle contraction. In-line with these results glycerophosphocolines have been previously reported to be elevated in people with T2D compared to normoglycaemic individuals in a small case-control study that employed quantitative phosphorous-31 magnetic resonance spectroscopy (^{31}P-MRS) (57).

The top three down regulated metabolites identified in this current study included; mannose - a carbohydrate involved in fructose, mannose and galactose metabolism, fructosyllysine an amino acid sub-class involved in lysine metabolism, and pyruvate a carbohydrate involved in glycolysis, gluconeogenesis, and pyruvate metabolism. The down regulation of carbohydrate (glucose) metabolism is plausible in the patient group given the insulin-resistant and hyperglycaemic environment of T2D. This elevated lipid metabolism and reduced glucose metabolism has been previously reported within the skeletal muscle of people with T2D *vs.* healthy controls (58). Moreover, the reciprocal relationship between glucose and fatty acids has been well described i.e., glucose oxidation is promoted by rising glucose levels, glucose and fatty acid storage, and inhibition of fatty acid oxidation, *vs.* elevated fatty acid levels promoting fatty acid oxidation and storage, and inhibiting glucose oxidation (59).

The upregulation of lysine metabolism has also been reported to be associated with increased risk of cardiovascular disease in those with established T2D from data reported from the PREDIMED study (60). The mechanisms at play here are not well understood but it is thought that lysine catabolism provides an alternative substrate(s) to glucose as a compensatory process, to increase

insulin secretion and maintain glucose homeostasis in the presence of early insulin resistance (61).

5.1.2 Pathway and enrichment analysis

The second objective of this study was to identify metabolic pathways that are differentially regulated in Stage A/B HF. The enrichment analysis identified a number of amino-acid metabolic pathways to be overrepresented in this cohort. The top hit was glycine, serine and threonine metabolism which is involved in protein synthesis, the synthesis of important biomolecules e.g.; nucleotides, and energy metabolism – specifically one-carbon metabolism. The latter involves the transfer of one-carbon units (methyl groups) for biosynthetic reactions, e.g.; methionine regeneration. Glycine, which is largely synthesised from serine and threonine (62), is a well-recognised plasma marker for metabolic diseases associated with obesity as described in this recent review by Alves *et al* (63).

Cysteine and methionine metabolism was the next enriched pathway. Methionine is an essential amino-acid and a precursor of cysteine (64), both are sulphur-containing amino-acids and cysteine itself is a precursor of the antioxidant glutathione, and taurine. The dysregulation of this amino-acid pathway, namely elevated circulating plasma levels of both amino-acids, have been shown to be positively associated with body mass index (BMI), fat mass, insulin resistance and the lipogenic enzyme, stearoyl coenzyme A desaturase (SCD) activity, in human observational studies (65-67). Thus, in support of the findings reported here given the baseline patient characteristics of obesity and insulin resistance. Furthermore, it has been recently reported that long-term excessive dietary intake of these sulphur containing amino-acids has been associated with increased risk of developing T2D (68). Data from the Third National Examination and Nutritional Health Survey (NHANES III) Study (1988-1994), which included some 11,576 participants, found, from their multivariate analysis, that higher consumption of methionine and cysteine (above the estimated average requirement) was independently associated with significant increase in their composite cardiometabolic disease risk score (69). These

sulphur containing amino-acids are found in an array of proteinaceous foods e.g.; eggs, beef, chicken *etc.* However, dietary content was not collected in this study but it may be important in future studies to identify those that have diets high in these amino-acids. It may offer a potential treatment strategy with dietary restriction of methionine (and thus its catabolic derivative cysteine), in several animal models, demonstrating improvements in glucose tolerance, insulin sensitivity, reduce inflammation and mediation of *de novo* lipid metabolism (70).

The third most enriched amino-acid pathway identified is arginine and proline metabolism. Arginine is a semi-essential functional ammino-acid formed *de novo* from glutamine/glutamate and proline in humans. However, across the life-cycle these synthetic pathways do not provide sufficient Arginine and therefore it is required from the diet at specific timepoints (71). It is an essential substrate for both nitric oxide (NO) synthesis and maintenance of the urea cycle where in its active state detoxifies ammonia. NO is a major vasodilator and important for vascular tone, and thus critical for healthy blood flow in and to tissues, it is involved in neurotransmission, and it has an important and versatile role in the innate immune response namely inflammation (72).

Perturbations in arginine metabolism can lead to impaired NO synthase activity and thus insulin resistance which has been previously shown within the skeletal tissue of adults with T2D (73). The mechanism is thought to be via a reduction in the NO enhancement of glucose transporter proteins (GLUT4) translocation to the cell membrane and/or NO interplay with proinflammatory adipokines. Furthermore, a central feature of endothelial dysfunction and inflammation is loss of NO generation (74). Endothelial dysfunction itself plays a critical and well defined role in the pathogenesis of diabetic vascular disease (75). Proline on the other hand is a non-essential amino acid, synthesised from glutamate, and has key roles in the biosynthesis of collagen (76) which is critical for connective tissue integrity e.g.; blood vessels, and in the maintenance of cellular redox homeostasis. The intracellular catabolism of proline can generate ATP and reactive oxygen species (ROS) (77). Collectively, dysregulated arginine and

proline metabolism lends itself to the sub-clinical pro-inflammatory and oxidative state that underpins T2D which drives insulin resistance and vascular dysfunction (78; 79).

Following the enrichment step the pathway analysis was conducted which essentially maps, by way of network analysis, the enriched metabolites onto related pathways. In networking the metabolites, you can visualise how they fit into the larger metabolic context. The pathway analysis is consistent with the differential expression analysis i.e.; glycerophospholipid metabolism is featured, and with the enrichment analysis with the identification of cysteine and methionine metabolism. These two metabolic pathways featured within the top five metabolic pathways identified and thus provides additional confidence in the robustness of the results reported here.   Another noteworthy, pathway identified within the top five is that of sphingolipid metabolism. The dysregulation of sphingolipid (and ceramide) metabolism has a purported cardiotoxic role in the pathogenesis of HF (80-83). Furthermore, these complex lipid species have been found to be associated with increased risk of T2D beyond traditional risk factors e.g.; age, physical activity, socioeconomic and smoking status *etc* in humans (84) and consistently shown, in animal models, to have a role in obesity-associated metabolic dysfunction (85).   The potential significance of; 1) glycerophospholipid metabolism, 2) cysteine and methionine metabolism and 3) sphingolipid metabolism in the progression of HF in obese adults with stage A/B HF warrants further investigation and validation in external cohorts.

5.1.3 Correlation analysis

The correlation analysis, between the cardiovascular structure and function outcomes of importance and peak VO_2 (a measure of exercise capacity), refined the candidate biomarkers down from 92 to 48 having potential added importance in the pathophysiology of T2D-related HF. These results demonstrated high representation again from the glycerophospholipid family and the sphingolipid and ceramide species, indicating these biomarkers may represent an early signal and potential targets in the prevention of HF in those

in stage A/B HF or therapeutic targets for ameliorating symptoms in the latter stages of the disease. However, this requires validation in external cohorts and further analysis to include adjustment for potential confounders in larger sample sizes. Moreover, cross-sectional analysis cannot confer causality, this can only be deduced through well designed interventional studies with post-intervention data collection, such as conducted in this project which is discussed below.

5.2 Pre-, post-MRP

5.2.1 Impact of MRP on metabolic signature

A total of twenty-four stage A/B HF participants randomised to the MRP arm completed the 12-week intervention achieving significant weight-loss and normalisation of glycaemic control. There was also evidence of reverse cardiac remodelling and improved exercise capacity in this group. The third objective of this study was to determine if the previously identified metabolic signature moved towards the "*healthy status*" following this MRP induced significant weight-loss. Here, I report the metabolic profiles to be partially discriminated between the two time points, and whilst no systematic transformation could be visualised across the metabolome, there were 47 differentially expressed metabolites of which eleven were common across the two analyses (case-control and pre-, post-MRP). These include metabolites featured in glycerophospholipid metabolism, sphingolipid/ceramide metabolism and amino-acid metabolism including glycine, serine and threonine metabolism which is consistent with findings from the case-control analysis. Ten of the eleven appear to migrate towards normal levels following the intervention when visualising the data in its simple box and whisker form. In summary, in this stage A/B HF (asymptomatic T2D) cohort their metabolic signature is characterised by three metabolic pathways; 1) glycerophospholipid metabolism, 2) sphingolipid/ceramide metabolism and 3) amino-acid metabolism namely glycine, serine and threonine metabolism. Their associated circulating plasma metabolites appear to shift towards the healthy status following significant weight-loss and normalisation of glycaemic control.

5.2.2 Candidate biomarkers and cardiovascular structure and function

The final objective of this project was to determine which metabolites (candidate biomarkers) are associated with indices of cardiovascular structure and function and exercise capacity. However, across the eleven candidate biomarkers there were number of weak correlations between the change in the outcomes of interest and only one co-efficient, of statistical significance, achieving a moderate score. This was for a positive association between the change in circulating levels of tartronate and change in LV EDVi. Tartronate is classified as a xenobiotic, representing exogenous chemicals. In this context, it is presumed to be present in the body through dietary consumption, likely originating from plant-based food sources (86). The mechanism by which this metabolite, whose circulating levels increase following the MRP, may induce greater end diastolic volume i.e.; greater LV elasticity, is not clear. It is plausible, and is hypothesised here, that the overall improvement in the patient's diet i.e.; 90% had reintroduction of food at eight weeks, with a diet plan advised by the study dietician, may account for an increase in this xenobiotic. Whilst the increase in this xenobiotic appears to align with the concurrent increase in LV EDVi (Left Ventricular End-Diastolic Volume indexed), it might be more a coincidental correlation rather than a directly causative mechanism at play. As previously stated, diet dairies were not included in this study and therefore this cannot be confirmed. Due to there being no convincing signal between changes in these metabolites and changes in the outcomes of interest, exploring whether or not they were more related to the key cardiometabolic changes that were observed following the diet was undertaken. The change in plasma levels of a number metabolites were indeed found to be moderately correlated with a number of the cardiometabolic indices. Notable linear relationships are observed for; the change in weight and change in hydroxybutyroylglycine, change in HbA1c and change in stearoyl-sphinganine and between change in fasting glucose and change in carboxyethylphenylalanine. Therefore, it is concluded that these candidate biomarkers are, and perhaps not surprisingly, associated with the significant weight reduction and improvement in glycaemic control observed in this cohort of asymptomatic T2D, and perhaps we are too

early in the disease course for a true and meaningful metabolic signal to be identified for stage A/B HF. On the other hand, it's possible that plasma might not be the optimal medium for examining metabolic perturbations in early HF. Indeed, in a recent metabolomic study of HFpEF (Stage C/D HF) whilst ketones, and metabolites of both the tricarboxylic acid cycle and branched-chain amino acids were found to be lower in endomyocardial biopsies compared to donor controls without HF, this was not mirrored in the plasma metabolome (87).

5.3 Strengths and limitations

The major strength and novelty of this study is that we utilised samples from participants in the DIASTOLIC randomised controlled trial, with well-balanced group allocation in addition to matched healthy controls at baseline. The metabolomic data analyses was conducted blinded to group allocation. To the best of our knowledge this is the first metabolomic analysis of a lifestyle intervention in people with asymptomatic T2D with Stage A/B HF classification that includes detailed cardiovascular structural and functional phenotyping with the gold standard technique of CMR. However, we acknowledge that the main limitation relates to this study being a post-hoc analysis with limited sample size and not including all groups of the RCT due to limited funding. To this point it is plausible that the change in metabolome following the intervention did not associate with reverse cardiac remodelling biomarkers, as assessed by CMR, because of the limited sample size or indeed because the exposure to the MRP was insufficient to measurably impact myocardial and cardiovascular status. Metabolomic studies are a "*snap-shot*" in time and cannot deduce the cause for the observed levels i.e.; a metabolite could be lower because of decreased production, higher degradation and /or uptake, or both. Furthermore, circulating levels may not reflect myocardial concentrations, which are incredibly difficult to obtain from asymptomatic individuals. Finally, a strength of this work is the adherence of Metabolon to the guidelines set by the NIH's Metabolomics Quality Assurance & Quality Control Consortium (mQACC)(88; 89), and their methodology and practices aligning with levels 1 and 2 of the metabolite identification levels (90).

However, Level 2 includes "*probable identification*" via a spectral library match and/or diagnostic evidence and not confirmed structures, as in Level 1, by use of for example a reference standard. The data provided by Metabolon is not granular enough to differentiate those metabolites that were identified via level 1 and those via level 2. Therefore the results reported, namely specific metabolite IDs/chemical formulae/structural information, should be further confirmed by other techniques such as tandem mass spectrometry (MS2 or MSn).

5.4 Future Research

These results require confirmation in a larger cohort of patients with a greater exposure to the MRP and/or longer follow-up assessments. Cross-sectional cohort studies remain relevant however, they should be longitudinal and include HF related outcomes and/or include intervention(s) to determine causality. It is important to ascertain if there are differential responses to interventions, such as MRP, by sex and or ethnic groups which may be masking the true interactions between metabolic pathways and measures of cardiovascular structure and function and exercise capacity. Moreover, augmenting or complementing these investigations with additional omics analyses, such as proteomics and transcriptomics, and/or different tissue samples/biofluids could potentially yield greater relevance and offer a deeper understanding of the fundamental pathogenic mechanisms that underlie the transition from stage A/B to stage C/D heart failure.

5.5 Conclusions

This project sought to determine if people with asymptomatic T2D, and therefore stage A/B HF, had a unique metabolic signature, with differentially regulated pathways, and examine the impact of a weight-reducing dietary intervention. Further, to determine which metabolites, if identified, were associated with indices of cardiovascular structure and function, and exercise capacity. It is reported, that in this cohort, a distinct metabolic signature can be described that is characterised by differential regulation of three key metabolic pathways; 1) glycerophospholipid metabolism, 2) sphingolipid/ceramide

metabolism and 3) amino-acid metabolism namely glycine, serine and threonine metabolism. Their associated circulating plasma metabolites appear to shift towards the "*healthy status*" following significant weight-loss and normalisation of glycaemic control. However, in this cohort the change in circulating plasma levels of the identified candidate biomarkers were not associated with changes in the key measures of cardiovascular structure and function nor exercise capacity, rather they appear to be associated with the significant weight reduction and improvement in glycaemic control observed. Conceivably, it may be too early in the disease course for a true and meaningful metabolic signal to be identified for stage A/B HF. Moreover, it is likely that alterations in the metabolome would be associated with indices of reverse cardiac remodelling in a larger sample size that had a longer exposure to the intervention. These results require confirmation in larger external cohorts with longer exposure to the MRP and longer-term follow-up.

References

1. McDonagh TA, Metra M, Adamo M, Gardner RS, Baumbach A, Böhm M, Burri H, Butler J, Čelutkienė J, Chioncel O, Cleland JGF, Coats AJS, Crespo-Leiro MG, Farmakis D, Gilard M, Heymans S, Hoes AW, Jaarsma T, Jankowska EA, Lainscak M, Lam CSP, Lyon AR, McMurray JJV, Mebazaa A, Mindham R, Muneretto C, Francesco Piepoli M, Price S, Rosano GMC, Ruschitzka F, Kathrine Skibelund A, Group ESD. 2021 ESC Guidelines for the diagnosis and treatment of acute and chronic heart failure: Developed by the Task Force for the diagnosis and treatment of acute and chronic heart failure of the European Society of Cardiology (ESC) With the special contribution of the Heart Failure Association (HFA) of the ESC. European Heart Journal 2021;42:3599-3726

2. Conrad N, Judge A, Tran J, Mohseni H, Hedgecott D, Crespillo AP, Allison M, Hemingway H, Cleland JG, McMurray JJV, Rahimi K. Temporal trends and patterns in heart failure incidence: a population-based study of 4 million individuals. The Lancet 2018;391:572-580

3. NICE (Ed.). *Resource impact report: Chronic heart failure in adults: diagnosis and management (NG106)*. https://www.nice.org.uk/guidance, 2018

4. Barasa A, Schaufelberger M, Lappas G, Swedberg K, Dellborg M, Rosengren A. Heart failure in young adults: 20-year trends in hospitalization, aetiology, and case fatality in Sweden. Eur Heart J 2014;35:25-32

5. Roger VL. Epidemiology of heart failure. Circ Res 2013;113:646-659

6. Benjamin EJ, Virani SS, Callaway CW, Chamberlain AM, Chang AR, Cheng S, Chiuve SE, Cushman M, Delling FN, Deo R, de Ferranti SD, Ferguson JF, Fornage M, Gillespie C, Isasi CR, Jiménez MC, Jordan LC, Judd SE, Lackland D, Lichtman JH, Lisabeth L, Liu S, Longenecker CT, Lutsey PL, Mackey JS, Matchar DB, Matsushita K, Mussolino ME, Nasir K, O'Flaherty M, Palaniappan LP, Pandey A, Pandey DK, Reeves MJ, Ritchey MD, Rodriguez CJ, Roth GA, Rosamond WD, Sampson UKA, Satou GM, Shah SH, Spartano NL, Tirschwell DL, Tsao CW, Voeks JH, Willey JZ, Wilkins JT, Wu JH, Alger HM, Wong SS, Muntner P. Heart Disease and Stroke Statistics-2018 Update: A Report From the American Heart Association. Circulation 2018;137:e67-e492

7. Dunlay SM, Roger VL, Redfield MM. Epidemiology of heart failure with preserved ejection fraction. Nature Reviews Cardiology 2017;14:591-602

8. Tsao CW, Lyass A, Enserro D, Larson MG, Ho JE, Kizer JR, Gottdiener JS, Psaty BM, Vasan RS. Temporal Trends in the Incidence of and Mortality Associated With Heart Failure With Preserved and Reduced Ejection Fraction. JACC Heart Fail 2018;6:678-685

9. Shah KS, Xu H, Matsouaka RA, Bhatt DL, Heidenreich PA, Hernandez AF, Devore AD, Yancy CW, Fonarow GC. Heart Failure With Preserved, Borderline, and Reduced Ejection Fraction: 5-Year Outcomes. J Am Coll Cardiol 2017;70:2476-2486

10. Lam CSP, Gamble GD, Ling LH, Sim D, Leong KTG, Yeo PSD, Ong HY, Jaufeerally F, Ng TP, Cameron VA, Poppe K, Lund M, Devlin G, Troughton R, Richards AM, Doughty RN. Mortality associated with heart failure with preserved vs. reduced ejection fraction in a prospective international multi-ethnic cohort study. European Heart Journal 2018;39:1770-1780

11. Roger VL. Epidemiology of Heart Failure: A Contemporary Perspective. Circ Res 2021;128:1421-1434

12. Teramoto K, Teng TK, Chandramouli C, Tromp J, Sakata Y, Lam CS. Epidemiology and Clinical Features of Heart Failure with Preserved Ejection Fraction. Card Fail Rev 2022;8:e27

13. Owan TE, Hodge DO, Herges RM, Jacobsen SJ, Roger VL, Redfield MM. Trends in Prevalence and Outcome of Heart Failure with Preserved Ejection Fraction. New England Journal of Medicine 2006;355:251-259

14. Redfield MM, Borlaug BA. Heart Failure With Preserved Ejection Fraction: A Review. JAMA 2023;329:827-838

15. Zile MR, Baicu CF, Gaasch WH. Diastolic Heart Failure — Abnormalities in Active Relaxation and Passive Stiffness of the Left Ventricle. New England Journal of Medicine 2004;350:1953-1959

16. Borlaug BA. The pathophysiology of heart failure with preserved ejection fraction. Nat Rev Cardiol 2014;11:507-515

17. DeVore AD, McNulty S, Alenezi F, Ersboll M, Vader JM, Oh JK, Lin G, Redfield MM, Lewis G, Semigran MJ, Anstrom KJ, Hernandez AF, Velazquez EJ. Impaired left ventricular global longitudinal strain in patients with heart failure with preserved ejection fraction: insights from the RELAX trial. Eur J Heart Fail 2017;19:893-900

18. Karagodin I, Aba-Omer O, Sparapani R, Strande JL. Aortic stiffening precedes onset of heart failure with preserved ejection fraction in patients with asymptomatic diastolic dysfunction. BMC Cardiovascular Disorders 2017;17:62

19. Bilak JM, Alam U, Miller CA, McCann GP, Arnold JR, Kanagala P. Microvascular Dysfunction in Heart Failure with Preserved Ejection Fraction: Pathophysiology, Assessment, Prevalence and Prognosis. Card Fail Rev 2022;8:e24

20. Ding N, Shah AM, Blaha MJ, Chang PP, Rosamond WD, Matsushita K. Cigarette Smoking, Cessation, and Risk of Heart Failure With Preserved and Reduced Ejection Fraction. J Am Coll Cardiol 2022;79:2298-2305

21. Borlaug BA, Jensen MD, Kitzman DW, Lam CSP, Obokata M, Rider OJ. Obesity and heart failure with preserved ejection fraction: new insights and pathophysiological targets. Cardiovascular Research 2022;118:3434-3450

22. Lee DS, Gona P, Vasan RS, Larson MG, Benjamin EJ, Wang TJ, Tu JV, Levy D. Relation of Disease Pathogenesis and Risk Factors to Heart Failure With Preserved or Reduced Ejection Fraction. Circulation 2009;119:3070-3077

23. Gong FF, Jelinek MV, Castro JM, Coller JM, McGrady M, Boffa U, Shiel L, Liew D, Wolfe R, Stewart S, Owen AJ, Krum H, Reid CM, Prior DL, Campbell DJ. Risk factors for incident heart failure with preserved or reduced ejection fraction, and valvular heart failure, in a community-based cohort. Open Heart 2018;5:e000782

24. Ceriello A, Catrinoiu D, Chandramouli C, Cosentino F, Dombrowsky AC, Itzhak B, Lalic NM, Prattichizzo F, Schnell O, Seferović PM, Valensi P, Standl E, the D, Group CES. Heart failure in type 2 diabetes: current perspectives on screening, diagnosis and management. Cardiovasc Diabetol 2021;20:218

25. Aronow WS, Ahn C. Incidence of heart failure in 2,737 older persons with and without diabetes mellitus. Chest 1999;115:867-868

26. Bertoni AG, Tsai A, Kasper EK, Brancati FL. Diabetes and idiopathic cardiomyopathy: a nationwide case-control study. Diabetes Care 2003;26:2791-2795

27. Maisch B, Alter P, Pankuweit S. Diabetic cardiomyopathy--fact or fiction? Herz 2011;36:102-115

28. Bozkurt B, Coats AJ, Tsutsui H, Abdelhamid M, Adamopoulos S, Albert N, Anker SD, Atherton J, Böhm M, Butler J, Drazner MH, Felker GM, Filippatos G, Fonarow GC, Fiuzat M, Gomez-Mesa JE, Heidenreich P, Imamura T, Januzzi J, Jankowska EA, Khazanie P, Kinugawa K, Lam CSP, Matsue Y, Metra M, Ohtani T, Francesco Piepoli M, Ponikowski P, Rosano GMC, Sakata Y, Seferović P, Starling RC, Teerlink JR, Vardeny O, Yamamoto K, Yancy C, Zhang J, Zieroth S. Universal Definition and Classification of Heart Failure: A Report of the Heart Failure Society of America, Heart Failure

Association of the European Society of Cardiology, Japanese Heart Failure Society and Writing Committee of the Universal Definition of Heart Failure. J Card Fail 2021;

29. McHugh K, DeVore AD, Wu J, Matsouaka RA, Fonarow GC, Heidenreich PA, Yancy CW, Green JB, Altman N, Hernandez AF. Heart Failure With Preserved Ejection Fraction and Diabetes: JACC State-of-the-Art Review. Journal of the American College of Cardiology 2019;73:602-611

30. Rubler S, Dlugash J, Yuceoglu YZ, Kumral T, Branwood AW, Grishman A. New type of cardiomyopathy associated with diabetic glomerulosclerosis. The American Journal of Cardiology 1972;30:595-602

31. Seferović PM, Paulus WJ. Clinical diabetic cardiomyopathy: a two-faced disease with restrictive and dilated phenotypes. European Heart Journal 2015;36:1718-1727

32. Gulsin GS, Athithan L, McCann GP. Diabetic cardiomyopathy: prevalence, determinants and potential treatments. Ther Adv Endocrinol Metab 2019;10:2042018819834869

33. Athithan L, Gulsin GS, McCann GP, Levelt E. Diabetic cardiomyopathy: Pathophysiology, theories and evidence to date. World J Diabetes 2019;10:490-510

34. Lorenzo-Almorós A, Cepeda-Rodrigo JM, Lorenzo Ó. Diabetic cardiomyopathy. Revista Clínica Española (English Edition) 2022;222:100-111

35. Goldin A, Beckman JA, Schmidt AM, Creager MA. Advanced Glycation End Products. Circulation 2006;114:597-605

36. Longo M, Zatterale F, Naderi J, Parrillo L, Formisano P, Raciti GA, Beguinot F, Miele C. Adipose Tissue Dysfunction as Determinant of Obesity-Associated Metabolic Complications. Int J Mol Sci 2019;20

37. Brady EM, Gulsin GS, Mirkes EM, Parke K, Kanagala P, Ng LL, Graham-Brown MPM, Athithan L, Henson J, Redman E, Yang J, Zhao L, Argyridou S, Gray LJ, Yates T, Davies MJ, McCann GP. Fibro-inflammatory recovery and type 2 diabetes remission following a low calorie diet but not exercise training: A secondary analysis of the DIASTOLIC randomised controlled trial. Diabet Med 2022;39:e14884

38. Paulus WJ, Zile MR. From Systemic Inflammation to Myocardial Fibrosis. Circulation Research 2021;128:1451-1467

39. Sutanto H, Lyon A, Lumens J, Schotten U, Dobrev D, Heijman J. Cardiomyocyte calcium handling in health and disease: Insights from in vitro and in silico studies. Progress in Biophysics and Molecular Biology 2020;157:54-75

40. Dattani A, Joshi S, Yeo JL, Singh A, Brady EM, Parke KS, Arnold JR, Singh T, Kershaw LE, Spath NB, Reynolds RM, Forbes S, Gibb FW, Semple SI, Dweck MR, Newby DE, McCann GP, Gulsin GS. Impaired Myocardial Calcium Uptake in Patients With Diabetes Mellitus: A Manganese-Enhanced Cardiac Magnetic Resonance Study. JACC: Cardiovascular Imaging 2023;

41. Shah K, Seeley S, Schulz C, Fisher J, Gururaja Rao S. Calcium Channels in the Heart: Disease States and Drugs. Cells 2022;11

42. Taegtmeyer H, Young ME, Lopaschuk GD, Abel ED, Brunengraber H, Darley-Usmar V, Rosiers CD, Gerszten R, Glatz JF, Griffin JL, Gropler RJ, Holzhuetter H-G, Kizer JR, Lewandowski ED, Malloy CR, Neubauer S, Peterson LR, Portman MA, Recchia FA, Eyk JEV, Wang TJ. Assessing Cardiac Metabolism. Circulation Research 2016;118:1659-1701

43. Bayeva M, Sawicki KT, Ardehali H. Taking Diabetes to Heart—Deregulation of Myocardial Lipid Metabolism in Diabetic Cardiomyopathy. Journal of the American Heart Association 2013;2:e000433

44. Goodpaster BH, Sparks LM. Metabolic Flexibility in Health and Disease. Cell Metab 2017;25:1027-1036

45. Taegtmeyer H, McNulty P, Young ME. Adaptation and maladaptation of the heart in diabetes: Part I: general concepts. Circulation 2002;105:1727-1733

46. Lopaschuk GD, Karwi QG, Tian R, Wende AR, Abel ED. Cardiac Energy Metabolism in Heart Failure. Circ Res 2021;128:1487-1513

47. Reddy YNV, Rikhi A, Obokata M, Shah SJ, Lewis GD, AbouEzzedine OF, Dunlay S, McNulty S, Chakraborty H, Stevenson LW, Redfield MM, Borlaug BA. Quality of life in heart failure with preserved ejection fraction: importance of obesity, functional capacity, and physical inactivity. Eur J Heart Fail 2020;22:1009-1018

48. NICE (Ed.). *Dapagliflozin for treating chronic heart failure with preserved or mildly reduced ejection fraction [ID1648]*. nice.org.uk, 2023

49. Anker SD, Butler J, Filippatos G, Ferreira JP, Bocchi E, Böhm M, Brunner–La Rocca H-P, Choi D-J, Chopra V, Chuquiure-Valenzuela E, Giannetti N, Gomez-Mesa JE, Janssens S, Januzzi JL, Gonzalez-Juanatey JR, Merkely B, Nicholls SJ, Perrone SV, Piña IL, Ponikowski P, Senni M, Sim D, Spinar J, Squire I, Taddei S, Tsutsui H, Verma S, Vinereanu D, Zhang J, Carson P, Lam CSP, Marx N, Zeller C, Sattar N, Jamal W, Schnaidt S, Schnee JM, Brueckmann M, Pocock SJ, Zannad F, Packer M. Empagliflozin in Heart Failure with a Preserved Ejection Fraction. New England Journal of Medicine 2021;385:1451-1461

50. Solomon SD, McMurray JJV, Claggett B, de Boer RA, DeMets D, Hernandez AF, Inzucchi SE, Kosiborod MN, Lam CSP, Martinez F, Shah SJ, Desai AS, Jhund PS, Belohlavek J, Chiang C-E, Borleffs CJW, Comin-Colet J, Dobreanu D, Drozdz J, Fang JC, Alcocer-Gamba MA, Al Habeeb W, Han Y, Cabrera Honorio JW, Janssens SP, Katova T, Kitakaze M, Merkely B, O'Meara E, Saraiva JFK, Tereshchenko SN, Thierer J, Vaduganathan M, Vardeny O, Verma S, Pham VN, Wilderäng U, Zaozerska N, Bachus E, Lindholm D, Petersson M, Langkilde AM. Dapagliflozin in Heart Failure with Mildly Reduced or Preserved Ejection Fraction. New England Journal of Medicine 2022;387:1089-1098

51. Gulsin GS, Swarbrick DJ, Athithan L, Brady EM, Henson J, Baldry E, Argyridou S, Jaicim NB, Squire G, Walters Y, Marsh A-M, McAdam J, Parke KS, Biglands JD, Yates T, Khunti K, Davies MJ, McCann GP. Effects of Low-Energy Diet or Exercise on Cardiovascular Function in Working-Age Adults With Type 2 Diabetes: A Prospective, Randomized, Open-Label, Blinded End Point Trial. Diabetes Care 2020;43:1300-1310

52. Zhang H-W, Lv C, Zhang L-J, Guo X, Shen Y-W, Nagle DG, Zhou Y-D, Liu S-H, Zhang W-D, Luan X. Application of omics- and multi-omics-based techniques for natural product target discovery. Biomedicine & Pharmacotherapy 2021;141:111833

53. Gulsin GS, Brady EM, Swarbrick DJ, Athithan L, Henson J, Baldry E, McAdam J, Marsh A-M, Parke KS, Wormleighton JV, Levelt E, Yates T, Bodicoat D, Khunti K, Davies MJ, McCann GP. Rationale, design and study protocol of the randomised controlled trial: Diabetes Interventional Assessment of Slimming or Training tO Lessen Inconspicuous Cardiovascular Dysfunction (the DIASTOLIC study). BMJ Open 2019;9:e023207

54. EFSA NDA Panel (EFSA Panel on Dietetic Products NaA. Scientific Opinion on the essential composition of total diet replacements for weight control. EFSA Journal 2015;13:52

55. Xia J, Wishart DS. Metabolomic Data Processing, Analysis, and Interpretation Using MetaboAnalyst. Current Protocols in Bioinformatics 2011;34:14.10.11-14.10.48

56. Guasch-Ferré M, Hruby A, Toledo E, Clish CB, Martínez-González MA, Salas-Salvadó J, Hu FB. Metabolomics in Prediabetes and Diabetes: A Systematic Review and Meta-analysis. Diabetes Care 2016;39:833-846

57. Clarke G.D. VJ, Tripathy D. et al. . Increased glycerophosphocholine concentration is associated with insulin resistance and hyperglycaemia in skeletal muscle. In *European Association for the study of Diabetes* Berlin,

58. Falholt K, Jensen I, Jensen SL, Mortensen H, Vølund A, Heding LG, Petersen PN, Falholt W. Carbohydrate and Lipid Metabolism of Skeletal Muscle in Type 2 Diabetic Patients. Diabetic Medicine 1988;5:27-31

59. Randle PJ, Garland PB, Hales CN, Newsholme EA. THE GLUCOSE FATTY-ACID CYCLE ITS ROLE IN INSULIN SENSITIVITY AND THE METABOLIC DISTURBANCES OF DIABETES MELLITUS. The Lancet 1963;281:785-789

60. Razquin C, Ruiz-Canela M, Clish CB, Li J, Toledo E, Dennis C, Liang L, Salas-Huetos A, Pierce KA, Guasch-Ferré M, Corella D, Ros E, Estruch R, Gómez-Gracia E, Fitó M, Lapetra J, Romaguera D, Alonso-Gómez A, Serra-Majem L, Salas-Salvadó J, Hu FB, Martínez-González MA. Lysine pathway metabolites and the risk of type 2 diabetes and cardiovascular disease in the PREDIMED study: results from two case-cohort studies. Cardiovascular Diabetology 2019;18:151

61. Libert DM NA, Natowicz MR. Metabolomic analysis of obesity, metabolic syndrome, and type 2 diabetes: amino acid and acylcarnitine levels change along a spectrum of metabolic wellness. Peer J 2018;6:e5410

62. Ducker GS, Rabinowitz JD. One-Carbon Metabolism in Health and Disease. Cell Metab 2017;25:27-42

63. Alves A, Bassot A, Bulteau AL, Pirola L, Morio B. Glycine Metabolism and Its Alterations in Obesity and Metabolic Diseases. Nutrients 2019;11

64. Brosnan JT, Brosnan ME. The sulfur-containing amino acids: an overview. J Nutr 2006;136:1636s-1640s

65. Elshorbagy AK, Nurk E, Gjesdal CG, Tell GS, Ueland PM, Nygård O, Tverdal A, Vollset SE, Refsum H. Homocysteine, cysteine, and body composition in the Hordaland Homocysteine Study: does cysteine link amino acid and lipid metabolism?1. The American Journal of Clinical Nutrition 2008;88:738-746

66. Elshorbagy AK, Valdivia-Garcia M, Refsum H, Butte N. The Association of Cysteine with Obesity, Inflammatory Cytokines and Insulin Resistance in Hispanic Children and Adolescents. PLOS ONE 2012;7:e44166

67. Vinknes KJ, Dekker JM, Drevon CA, Refsum H, Nurk E, Nijpels G, Stehouwer CDA, Teerlink T, Tell GS, Nygård O, Vollset SE, Ueland PM, Elshorbagy AK. Plasma sulfur amino acids and stearoyl-CoA desaturase activity in two caucasian populations. Prostaglandins, Leukotrienes and Essential Fatty Acids 2013;89:297-303

68. Dong Z, Richie JP, Jr., Gao X, Al-Shaar L, Nichenametla SN, Shen B, Orentreich D. Cumulative Consumption of Sulfur Amino Acids and Risk of Diabetes: A Prospective Cohort Study. J Nutr 2022;152:2419-2428

69. Dong Z, Gao X, Chinchilli VM, Sinha R, Muscat J, Winkels RM, Richie JP, Jr. Association of sulfur amino acid consumption with cardiometabolic risk factors: Cross-sectional findings from NHANES III. EClinicalMedicine 2020;19:100248

70. Yin J, Ren W, Chen S, Li Y, Han H, Gao J, Liu G, Wu X, Li T, Woo Kim S, Yin Y. Metabolic Regulation of Methionine Restriction in Diabetes. Molecular Nutrition & Food Research 2018;62:1700951

71. Wu G, Meininger CJ, McNeal CJ, Bazer FW, Rhoads JM. Role of L-Arginine in Nitric Oxide Synthesis and Health in Humans. In *Amino Acids in Nutrition and Health: Amino Acids in Gene Expression, Metabolic Regulation, and Exercising Performance* Wu G, Ed. Cham, Springer International Publishing, 2021, p. 167-187

72. Tripathi P, Tripathi P, Kashyap L, Singh V. The role of nitric oxide in inflammatory reactions. FEMS Immunology & Medical Microbiology 2007;51:443-452

73. Kashyap SR, Roman LJ, Lamont J, Masters BSS, Bajaj M, Suraamornkul S, Belfort R, Berria R, Kellogg DL, Jr., Liu Y, DeFronzo RA. Insulin Resistance Is Associated with Impaired Nitric Oxide Synthase Activity in Skeletal Muscle of Type 2 Diabetic Subjects. The Journal of Clinical Endocrinology & Metabolism 2005;90:1100-1105

74. Cannon RO, 3rd. Role of nitric oxide in cardiovascular disease: focus on the endothelium. Clin Chem 1998;44:1809-1819

75. De Vriese AS, Verbeuren TJ, Van de Voorde J, Lameire NH, Vanhoutte PM. Endothelial dysfunction in diabetes. Br J Pharmacol 2000;130:963-974

76. Karna E, Szoka L, Huynh TYL, Palka JA. Proline-dependent regulation of collagen metabolism. Cell Mol Life Sci 2020;77:1911-1918

77. Vettore LA, Westbrook RL, Tennant DA. Proline metabolism and redox; maintaining a balance in health and disease. Amino Acids 2021;53:1779-1788

78. Pickup JC. Inflammation and Activated Innate Immunity in the Pathogenesis of Type 2 Diabetes. Diabetes Care 2004;27:813-823

79. Oguntibeju OO. Type 2 diabetes mellitus, oxidative stress and inflammation: examining the links. Int J Physiol Pathophysiol Pharmacol 2019;11:45-63

80. Ljubkovic M, Gressette M, Bulat C, Cavar M, Bakovic D, Fabijanic D, Grkovic I, Lemaire C, Marinovic J. Disturbed Fatty Acid Oxidation, Endoplasmic Reticulum Stress, and Apoptosis in Left Ventricle of Patients With Type 2 Diabetes. Diabetes 2019;68:1924-1933

81. Doenst T, Nguyen TD, Abel ED. Cardiac metabolism in heart failure: implications beyond ATP production. Circ Res 2013;113:709-724

82. Drosatos K, Schulze PC. Cardiac lipotoxicity: molecular pathways and therapeutic implications. Curr Heart Fail Rep 2013;10:109-121

83. Park TS, Hu Y, Noh HL, Drosatos K, Okajima K, Buchanan J, Tuinei J, Homma S, Jiang XC, Abel ED, Goldberg IJ. Ceramide is a cardiotoxin in lipotoxic cardiomyopathy. J Lipid Res 2008;49:2101-2112

84. Chen GC, Chai JC, Yu B, Michelotti GA, Grove ML, Fretts AM, Daviglus ML, Garcia-Bedoya OL, Thyagarajan B, Schneiderman N, Cai J, Kaplan RC, Boerwinkle E, Qi Q. Serum sphingolipids and incident diabetes in a US population with high diabetes burden: the Hispanic Community Health Study/Study of Latinos (HCHS/SOL). Am J Clin Nutr 2020;112:57-65

85. Holland WL, Summers SA. Sphingolipids, insulin resistance, and metabolic disease: new insights from in vivo manipulation of sphingolipid metabolism. Endocr Rev 2008;29:381-402

86. Rieben WK, Hastings AB. [Chemical and biological studies on tartronic acid]. Helv Physiol Pharmacol Acta 1946;4:52

87. Hahn VS, Petucci C, Kim M-S, Bedi KC, Wang H, Mishra S, Koleini N, Yoo EJ, Margulies KB, Arany Z, Kelly DP, Kass DA, Sharma K. Myocardial Metabolomics of Human Heart Failure With Preserved Ejection Fraction. Circulation 2023;147:1147-1161

88. Beger RD, Dunn WB, Bandukwala A, Bethan B, Broadhurst D, Clish CB, Dasari S, Derr L, Evans A, Fischer S, Flynn T, Hartung T, Herrington D, Higashi R, Hsu P-C, Jones C, Kachman M, Karuso H, Kruppa G, Lippa K, Maruvada P, Mosley J, Ntai I, O'Donovan C, Playdon M, Raftery D, Shaughnessy D, Souza A, Spaeder T, Spalholz B, Tayyari F, Ubhi B, Verma M, Walk T, Wilson I, Witkin K, Bearden DW, Zanetti KA. Towards quality assurance and quality control in untargeted metabolomics studies. Metabolomics 2019;15

89. Evans AM, O'Donovan C, Playdon M, Beecher C, Beger RD, Bowden JA, Broadhurst D, Clish CB, Dasari S, Dunn WB, Griffin JL, Hartung T, Hsu PC, Huan T, Jans J, Jones CM, Kachman M, Kleensang A, Lewis MR, Monge ME, Mosley JD, Taylor E, Tayyari F,

Theodoridis G, Torta F, Ubhi BK, Vuckovic D. Dissemination and analysis of the quality assurance (QA) and quality control (QC) practices of LC-MS based untargeted metabolomics practitioners. Metabolomics 2020;16:113

90. Schymanski EL, Jeon J, Gulde R, Fenner K, Ruff M, Singer HP, Hollender J. Identifying Small Molecules via High Resolution Mass Spectrometry: Communicating Confidence. Environmental Science & Technology 2014;48:2097-2098

Appendices

Appendix 1| Metabolite view of data normalisation case-control analysis
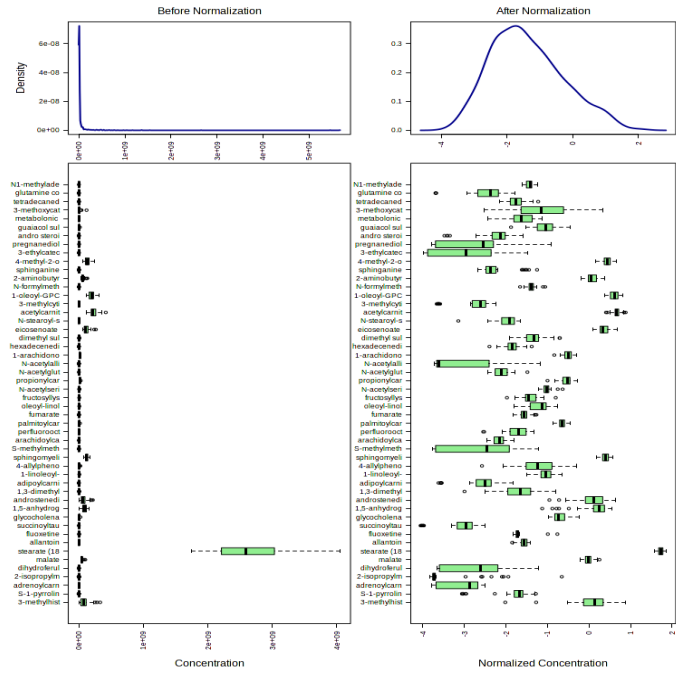
Appendix 2| Feature view of data before and after normalising pre-post analysis
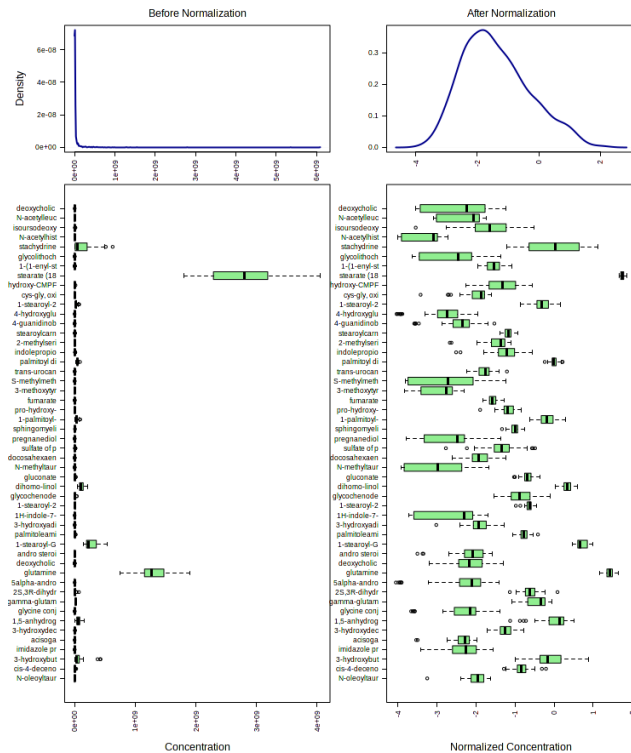
Appendix 3|Candidate biomarkers with significant adjusted fold change between groupsCandidate biomarkers with significant adjusted fold change between groups

METABOLITE	FC	LOG2(FC)	P.AJUSTED	SUPER-PATHWAY	SUB PATHWAY	DIRECTION
4-hydroxyglutamate	0.24067	-2.0549	7.74E-05	Amino acid	Glutamate metabolism	Down
n-stearoyl-sphinganine (d18:0/18:0)	0.31944	-1.6464	0.000941	Lipids	Dihydroceramides	Down
formiminoglutamate	0.33814	-1.5643	0.003648	Amino acid	Histidine Metabolism	Down
n-(2-furoyl)glycine	0.35428	-1.497	0.052766	Xenobiotics	Food Component/Plant	Down
1-carboxyethylphenylalanine	0.37634	-1.4099	0.001715	Amino acid	Phenylalanine Metabolism	Down
deoxycholic acid (12 or 24)-sulfate	0.3822	-1.3876	0.031131	Lipids	Secondary Bile Acid Metabolism	Down
taurodeoxycholate	0.38544	-1.3754	0.049448	Lipids	Secondary Bile Acid Metabolism	Down
dihydroferulic acid sulfate	0.41413	-1.2718	0.004874	Xenobiotics	Food Component/Plant	Down
cystathionine	0.43616	-1.1971	0.010428	Amino acid	Methionine, Cysteine, SAM and Taurine Metabolism	Down
butyrylcarnitine (c4)	0.48724	-1.0373	0.000295	Amino acid	Leucine, Isoleucine and Valine Metabolism	Down
(r)-3-hydroxybutyrylcarnitine	0.49015	-1.0287	0.056105	Lipids	Fatty Acid Metabolism (Acyl Carnitine, Hydroxy)	Down
8-methoxykynurenate	0.49335	-1.0193	0.022111	Amino acid	Tryptophan Metabolism	Down
glutamate	0.50404	-0.9884	3.77E-05	Amino acid	Glutamate metabolism	Down
taurochenodeoxycholate	0.50609	-0.98255	0.060098	Lipids	Primary Bile Acid Metabolism	Down
fructosyllysine	0.53733	-0.89611	3.07E-05	Amino acid	Lysine Metabolism	Down
1-palmitoleoylglycerol (16:1)	0.54221	-0.88308	0.04634	Lipids	Monoacylglycerol	Down
2-aminoadipate	0.54309	-0.88073	0.000247	Amino acid	Lysine Metabolism	Down
n-acetyltyrosine	0.54309	-0.88073	0.024727	Amino acid	Tyrosine Metabolism	Down
gamma-glutamylisoleucine	0.55187	-0.85761	0.012177	Peptide	Gamma-glutamyl Amino Acid	Down
docosatrienoate (22:3n6)	0.55556	-0.84799	0.002438	Lipids	Long Chain Polyunsaturated Fatty Acid (n3 and n6)	Down
linoleoyl-arachidonoyl-glycerol (18:2/20:4) [1]	0.56044	-0.83536	0.022622	Lipids	Diacylglycerol	Down
1-carboxyethylvaline	0.57189	-0.8062	0.003081	Amino acid	Leucine, Isoleucine and Valine Metabolism	Down
adrenate (22:4n6)	0.57747	-0.79218	0.000628	Lipids	Long Chain Polyunsaturated Fatty Acid (n3 and n6)	Down
1-dihomo-linolenylglycerol (20:3)	0.58344	-0.77735	0.081447	Lipids	Monoacylglycerol	Down
picolinoylglycine	0.59255	-0.75498	0.011068	Lipids	Fatty Acid Metabolism (Acyl Glycine)	Down
alpha-ketobutyrate	0.59341	-0.75289	0.017355	Amino acid	Methionine, Cysteine, SAM and Taurine Metabolism	Down
mannonate	0.59765	-0.74262	2.82E-08	Xenobiotics	Food Component/Plant	Down
pyruvate	0.60453	-0.72612	3.38E-05	Carbohydrate	Glycolysis, Gluconeogenesis, and Pyruvate Metabolism	Down
isovalerylcarnitine (c5)	0.60842	-0.71687	0.001578	Amino acid	Leucine, Isoleucine and Valine Metabolism	Down

oleoyl-arachidonoyl-glycerol (18:1/20:4) [2]	0.6086	-0.71643	0.049165	Lipids	Diacylglycerol	Down
azelate (c9-dc)	0.60917	-0.71508	0.004737	Lipids	Fatty Acid, Dicarboxylate	Down
ethylmalonate	0.61266	-0.70683	0.098798	Amino acid	Leucine, Isoleucine and Valine Metabolism	Down
mannose	0.617	-0.69665	2.82E-08	Carbohydrate	Fructose, Mannose and Galactose Metabolism	Down
oleoyl-arachidonoyl-glycerol (18:1/20:4) [1]	0.61907	-0.69182	0.043945	Lipids	Diacylglycerol	Down
docosatrienoate (22:3n3)	0.62066	-0.68813	0.000376	Lipids	Long Chain Polyunsaturated Fatty Acid (n3 and n6)	Down
ribitol	0.62659	-0.67441	0.000897	Carbohydrate	Pentose Metabolism	Down
metabolonic lactone sulfate	0.62723	-0.67294	0.068612	Partially Characterized Molecules	Partially Characterized Molecules	Down
linoleoyl-arachidonoyl-glycerol (18:2/20:4) [2]	0.62838	-0.67028	0.043945	Lipids	Diacylglycerol	Down
1-stearoyl-2-oleoyl-gpe (18:0/18:1)	0.63036	-0.66575	0.003074	Lipids	Phosphatidylethanolamine (PE)	Down
succinylcarnitine (c4-dc)	0.63648	-0.65181	0.022881	Energy	TCA cycle	Down
glucuronide of piperine metabolite c17h21no3 (4)	0.63836	-0.64756	0.094042	Xenobiotics	Food Component/Plant	Down
1-stearoyl-2-docosahexaenoyl-gpe (18:0/22:6)	0.65457	-0.61137	0.002443	Lipids	Phosphatidylethanolamine (PE)	Down
1-palmitoyl-2-oleoyl-gpe (16:0/18:1)	0.65567	-0.60896	0.018198	Lipids	Phosphatidylethanolamine (PE)	Down
linolenoylcarnitine (c18:3)	1.5013	0.58619	0.023131	Lipids	Fatty Acid Metabolism (Acyl Carnitine, Polyunsaturated)	Up
1-(1-enyl-palmitoyl)-2-palmitoyl-gpc (p-16:0/16:0)	1.5136	0.59795	2.47E-08	Lipids	Plasmalogen	Up
guanidinosuccinate	1.5192	0.60335	0.044574	Amino acid	Guanidino and Acetamido Metabolism	Up
oxalate (ethanedioate)	1.5399	0.62288	0.000867	Cofactors and Vitamins	Ascorbate and Aldarate Metabolism	Up
1-oleoyl-gpi (18:1)	1.5482	0.63064	0.005996	Lipids	Lysophospholipid	Up
dihomo-linolenoyl-choline	1.5716	0.65223	0.019696	Lipids	Fatty Acid Metabolism (Acyl Choline)	Up
1-stearoyl-2-linoleoyl-gpi (18:0/18:2)	1.5719	0.65253	0.003892	Lipids	Phosphatidylinositol (PI)	Up
3-hydroxybutyroylglycine	1.5786	0.65868	0.018659	Lipids	Fatty Acid Metabolism (Acyl Glycine)	Up
1-(1-enyl-palmitoyl)-gpc (p-16:0)	1.5812	0.66098	0.000941	Lipids	Lysoplasmalogen	Up
sphingomyelin (d17:1/14:0, d16:1/15:0)	1.5895	0.66857	0.000757	Lipids	Sphingomyelins	Up
1-(1-enyl-palmitoyl)-2-palmitoleoyl-gpc (p-16:0/16:1)	1.5919	0.67074	1.30E-05	Lipids	Plasmalogen	Up
1,5-anhydroglucitol (1,5-ag)	1.5972	0.67552	0.005207	Carbohydrate	Glycolysis, Gluconeogenesis, and Pyruvate Metabolism	Up
arachidonoylcholine	1.6134	0.69011	0.004226	Lipids	Fatty Acid Metabolism (Acyl Choline)	Up
1,2-dilinoleoyl-gpc (18:2/18:2)	1.6207	0.69657	0.000117	Lipids	Phosphatidylcholine (PC)	Up
lactosyl-n-nervonoyl-sphingosine (d18:1/24:1)	1.6218	0.69761	4.12E-06	Lipids	Lactosylceramides (LCER)	Up

n-delta-acetylornithine	1.6358	0.70999	0.014498	Amino acid	Urea cycle; Arginine and Proline Metabolism	Up
eicosenoylcarnitine (c20:1)	1.6517	0.72399	6.90E-05	Lipids	Fatty Acid Metabolism (Acyl Carnitine, Monounsaturated)	Up
arachidoylcarnitine (c20)	1.6545	0.7264	3.77E-05	Lipids	Fatty Acid Metabolism (Acyl Carnitine, Long Chain Saturated)	Up
glycosyl-n-nervonoyl-sphingosine (d18:1/24:1)	1.6581	0.7295	3.58E-05	Lipids	Hexosylceramides (HCER)	Up
2-ketocaprylate	1.675	0.74419	0.035972	Amino acid	Leucine, Isoleucine and Valine Metabolism	Up
n-acetylglycine	1.6971	0.76306	0.003756	Amino acid	Glycine, Serine and Threonine Metabolism	Up
1-(1-enyl-palmitoyl)-2-linoleoyl-gpc (p-16:0/18:2)	1.7096	0.77364	2.11E-08	Lipids	Plasmalogen	Up
3beta,7alpha-dihydroxy-5-cholestenoate	1.716	0.77909	0.007213	Lipids	Sterol	Up
trigonelline (n'-methylnicotinate)	1.7216	0.78378	0.075833	Cofactors and Vitamins	Nicotinate and Nicotinamide Metabolism	Up
pentose acid	1.7374	0.79694	0.07701	Partially Characterized Molecules	Partially Characterized Molecules	Up
1-(1-enyl-palmitoyl)-2-oleoyl-gpc (p-16:0/18:1)	1.798	0.84638	4.89E-09	Lipids	Plasmalogen	Up
branched chain 14:0 dicarboxylic acid	1.8117	0.85732	0.039131	Lipids	Fatty Acid, Dicarboxylate	Up
n-acetylhistidine	1.8283	0.87053	0.025514	Amino acid	Histidine Metabolism	Up
glycosyl ceramide (d18:2/24:1, d18:1/24:2)	1.8542	0.89082	5.16E-06	Lipids	Hexosylceramides (HCER)	Up
glycosyl-n-behenoyl-sphingadienine (d18:2/22:0)	1.8767	0.90817	2.68E-05	Lipids	Hexosylceramides (HCER)	Up
carotene diol (1)	1.8968	0.92355	1.96E-05	Cofactors and Vitamins	Vitamin A Metabolism	Up
histidine betaine (hercynine)	1.8994	0.92553	0.040635	Xenobiotics	Food Component/Plant	Up
stearoylcholine	1.9044	0.92931	0.000525	Lipids	Fatty Acid Metabolism (Acyl Choline)	Up
1-lignoceroyl-gpc (24:0)	1.9215	0.94224	6.36E-08	Lipids	Lysophospholipid	Up
indolepropionate	1.9232	0.94354	0.011433	Amino acid	Tryptophan Metabolism	Up
palmitoylcholine	1.9344	0.95187	0.000185	Lipids	Fatty Acid Metabolism (Acyl Choline)	Up
oleoylcholine	1.9537	0.96619	0.000473	Lipids	Fatty Acid Metabolism (Acyl Choline)	Up
tartronate (hydroxymalonate)	2.0025	1.0018	6.90E-05	Xenobiotics	Food Component/Plant	Up
docosahexaenoylcholine	2.0339	1.0242	0.000113	Lipids	Fatty Acid Metabolism (Acyl Choline)	Up
3-phenylpropionate (hydrocinnamate)	2.0397	1.0283	0.09424	Xenobiotics	Benzoate Metabolism	Up
carotene diol (2)	2.0759	1.0538	4.52E-07	Cofactors and Vitamins	Vitamin A Metabolism	Up
2-hydroxyoctanoate	2.0861	1.0608	0.020149	Lipids	Fatty Acid, Monohydroxy	Up
s-methylcysteine sulfoxide	2.1165	1.0817	0.050391	Amino acid	Methionine, Cysteine, SAM and Taurine Metabolism	Up

heme	2.1447	1.1008	0.080668	Cofactors and Vitamins	Hemoglobin and Porphyrin Metabolism	Up
carotene diol (3)	2.2205	1.1509	0.000153	Cofactors and Vitamins	Vitamin A Metabolism	Up
linoleoylcholine	2.256	1.1737	5.03E-05	Lipids	Fatty Acid Metabolism (Acyl Choline)	Up
1-linoleoyl-2-linolenoyl-gpc (18:2/18:3)	2.5914	1.3737	2.20E-06	Lipids	Phosphatidylcholine (PC)	Up
glycosyl ceramide (d18:1/23:1, d17:1/24:1)	3.2621	1.7058	0.007928	Lipids	Hexosylceramides (HCER)	Up
s-methylmethionine	3.5033	1.8087	0.013591	Amino acid	Methionine, Cysteine, SAM and Taurine Metabolism	Up
beta-cryptoxanthin	3.6845	1.8815	0.000173	Cofactors and Vitamins	Vitamin A Metabolism	Up
hydroxy-cmpf	4.5003	2.17	0.002341	Lipids	Fatty Acid, Dicarboxylate	Up
metabolite						
4-hydroxyglutamate	0.24067	-2.0549	7.74E-05	Amino acid	Glutamate metabolism	Down
n-stearoyl-sphinganine (d18:0/18:0)	0.31944	-1.6464	0.000941	Lipids	Dihydroceramides	Down
formiminoglutamate	0.33814	-1.5643	0.003648	Amino acid	Histidine Metabolism	Down
n-(2-furoyl)glycine	0.35428	-1.497	0.052766	Xenobiotics	Food Component/Plant	Down

Glycerophospholipid metabolism network plot

Cysteine and methionine metabolism network plot

Sphingolipid metabolism

Red boxes denote the metabolites from my candidate biomarkers